

POLITECNICO DI TORINO

Master degree in Electronic Engineering

Master's degree Thesis

**Optimization of NS-GAAFET technology through low- κ
dielectrics for spacer fabrication**



Supervisors

Prof. Gianluca Piccinini
M.Eng. Fabrizio Mo
M.Eng. Chiara Elfi Spano

Author

Antonio Colonna

Accademic year 2022-2023

Summary

Over the years, the manufacturing technology and structure of transistors have had continuous development. The channel length dimension has steadily decreased and the number of transistors per chip has steadily increased.

With the scaling and the considerable increase in the number of transistors, problems related to power consumption, transistor speed, interconnection delays and the achievement of channel lengths of a few nanometers problems such as the short channel effect (SCE) have had to be faced.

If the technological breakthrough of the last decade is represented by the FinFET which has made it possible to solve many problems thanks to the use of 3D technology, the next step is represented by the GAAFET, Gate All Around Field Effect Transistor. GAAFET technology with greater electrostatic control allowed scaling beyond 5 nm.

Unlike the FinFET, the spacer structure of the GAAFET is more complicated by having the inner spacers, dielectric material between the nanosheets to avoid short circuits between the gate and source and drain.

In the thesis, there is an overview of the GAAFET manufacturing processes focusing on the fabrication of the inner spacers which represent a fundamental and delicate step.

With the aim of improving the performance of GAAFETs, low dielectric constant(κ) materials have been analyzed. By implementing the low- κ materials both in the front-end-of-line and in the back-end-of-line it is possible to reduce the parasitic capacitances and consequently mainly reduce the power consumption and the RC delay.

In the More Moore chapter of IRDS 2022, it is predicted that the value of κ for spacers may reach 2.7 in 2034.

In the first phase, research analysis of low dielectric constant materials was conducted. The different types of materials, the mechanisms to further reduce the value of κ and the main problems were analyzed. It has been deduced that polymers are materials that have low dielectric constant and in general one can reduce the dielectric constant of a material through the creation of pores.

Low- κ materials have poor mechanical properties and this represents the major obstacle in implementation with current transistor fabrication processes.

Among the possible low- κ materials, the study of polytetrafluoroethylene (PTFE), a polymer with a κ value of about 2, was undertaken. Through the use of atomistic simulation software, QuantumATK, the main electrical and thermomechanical properties were simulated. In particular, the dielectric tensor, the glass transition temperature, the Young's modulus and the Poisson's ratio have been simulated.

In using this material as a dielectric for the GAAFETs, the focus is on the FEOL and in particular on its use as a spacer material.

The use of the Sentaurus software made it possible to simulate the GAAFET manufacturing processes and to check the performance of the device obtained. Then PTFE was introduced as a spacer material and through the simulation of the different parameters that characterize the performance of a transistor, the benefits of using a low- κ material were found.

Polymers represent a new frontier in their use as dielectric materials in transistors. Continuous research is needed into the perfect dielectric to be compatible with fabrication processes.

List of Figures

1.1	Spacer and inner spacer in GAAFET	12
1.2	Field lines of the electric dipole	13
1.3	Electronic polarization	14
1.4	Atomic or ionic polarization	14
1.5	Dipolar or orientational polarization	14
1.6	Interfacial polarization	15
1.7	A spectrum of electric permittivity at different frequencies	15
1.8	Possibilities for reducing the κ value of dielectrics.	17
1.9	classification scheme of low- κ dielectrics.	19
1.10	Representation of a tetrahedral silica unit (a) and the same unit of SiOCH material (b)	19
1.11	Representation of a silsesquioxane (SSQ) unit.	20
1.12	Dielectric constant as a function of porosity for different dielectrics.	21
1.13	classification scheme of porous low- κ materials.	22
1.14	Representative preparations for polymers of post-pore formation: (a) template method, and (b) etching method.	23
1.15	Young's modulus of low- κ films as a function of porosity.	25
1.16	Chain of polytetrafluoroethylene	28
2.1	Fabrication of Si-SiGe layers	32
2.2	Fabrication of dummy gate	33
2.3	Fabrication of spacer and inner spacer	34
2.4	S/D epitaxial growth	35
2.5	Fabrication of gate	36
2.6	Fabrication of contacts	37
2.7	Inner spacer formation	38
2.8	SiGe indentation process	39
2.9	Parasitic elements in the GAAFET	39
3.1	Design flow from QuantumATK to Sentaurus TCAD.	41
3.2	Design flow from atomic scale simulator to process design kit.	42
3.3	Structure of QuantumATK platform	42
3.4	The QuantumATK GUI.	43
3.5	Polymer Builder in the Script Generator	46

3.6	Polymer Environment in the Script Generator	47
3.7	Pre-equilibration in the Script Generator	47
3.8	Force Field in the Script Generator	48
3.9	Example: 20 chains with 20 monomers per each chain of Polytetrafluoroethylene with $2.2g/cm^3$ density.	49
3.10	Script of the dielectric tensor simulation	49
3.11	Dielectric constant of PTFE_2_1	51
3.12	Dielectric constant of PTFE_2_1 at low frequency	52
3.13	Real part of dielectric constant of PTFE_2_2 with density $2.2 g/cm^3$ at low frequency	53
3.14	Script of the glass transition temperature simulation	55
3.15	Molecular Dynamics parameters	55
3.16	Glass Transition Temperature Analyzer of PTFE	56
3.17	Young's modulus and Poisson ratio Script	57
3.18	Young's modulus and Poisson ratio MolecularDynamics	58
3.19	Young's modulus plot of PTFE	59
3.20	Poisson ratio plot of PTFE	60
3.21	Specific heat capacity of PTFE	61
4.1	Sentaurus TCAD suite	63
4.2	NS-GAAFET process flow	65
4.3	n-type GAAFET device at the end of the Sprocess simulation	67
4.4	I_D - V_{GS} curves of n-type NS-GAAFET in linear regime.	68
4.5	I_D - V_{GS} curves of n-type NS-GAAFET in saturation regime.	68
4.6	I_D - V_{GS} curves of n-type NS-GAAFET in saturation for different spacer materials	69
4.7	p-type GAAFET device at the end of the Sprocess simulation	70
4.8	I_D - V_{GS} curves of p-type NS-GAAFET in linear regime.	70
4.9	I_D - V_{GS} curves of p-type NS-GAAFET in saturation regime.	71
4.10	I_D - V_{GS} curves of p-type NS-GAAFET in saturation for different spacer materials	72
4.11	Small signal equivalent circuit NS-GAAFET a) ON-state , b) OFF-state	73

List of Tables

1.1	Time constant and characteristic frequency for the different polarization mechanisms.	16
1.2	Dielectric constants of polymers	27
1.3	Physical properties of PTFE	28
1.4	Mechanical properties of PTFE	28
1.5	Electical properties of PTFE	29
1.6	Thermal properties of PTFE	29
3.1	Monomer database QuantumATK	45
3.2	PTFE_2_2 dielectric constant with different density	53
3.3	Comparison of the dielectric constant between the different configurations of PTFE with a density of 2.2 g/cm^3	54
4.1	Sprocess NS-GAAFET parameters	65
4.2	Parameters of n-type NSGAAFET with different channel lengths	69
4.3	Parameters of p-type NSGAAFET with different channel lengths	71

List of acronyms

BEOL Back End Of Line.

CMOS Complementary Metal-Oxide-Semiconductor.

CMP Chemical Mechanical Polishing.

DIBL Drain-Induced Barrier Lowering.

ESL Etch Stop Layer.

FEOL Front End Of Line.

finFET Fin Field-Effect Transistor.

GAAFET Gate-All-Around Field-Effect Transistor.

ILD Inter layer dielectric.

IRDS International Roadmap for Devices and Systems.

LDD low doped drain.

NSGAAFET Nanosheet Gate-All-Around Field-Effect.

PSG Phosphosilicate Glass.

PTFE Polytetrafluoroethylene.

RIE Reactive Ion Etching.

RTA Rapid Thermal Annealing.

S/D Source/Drain.

SAC Self-Aligned Contact.

SCE Short Channel Effect.

SIT Sidewall Image Transfer.

SS Subthreshold Slope.

TCAD Technology Computer-Aided Design.

Contents

List of Figures	5
List of Tables	7
List of acronyms	8
1 Introduction	11
1.1 Dielectric material and dielectric constant	12
1.1.1 Low dielectric material	17
1.2 Polytetrafluoroethylene	26
2 V-Stacked nanosheet GAAFET	31
2.1 Fabrication processes	31
2.1.1 Fabrication of Si-SiGe layers	31
2.1.2 Dummy gate	32
2.1.3 Spacer and inner spacer formation	33
2.1.4 S/D epitaxial growth	34
2.1.5 Gate stack	35
2.1.6 Contacts	36
2.2 Inner spacer	37
2.3 Parasitic capacitance	39
3 Atomistic simulations in QuantumATK	41
3.1 Polymer Builder	44
3.1.1 Procedure of the Polymer Builder	45
3.1.2 Analyzing the electrical properties of a polymer material	49
3.1.3 Analyzing the thermo-mechanical properties of a polymer material	54
4 Device simulations in Sentaurus TCAD	63
4.1 NS-GAAFET simulation	65
4.1.1 n-type NS-GAAFET	67
4.1.2 p-type NS-GAAFET	70
4.2 NS-GAAFET frequency response	72
5 Conclusions and future research	75

A	Insight into QuantumATK classes	77
A.1	Dielectric tensor analysis Python script	77
A.2	Glass transition temperature Python script	80
A.3	Young's modulus and Poisson ratio Python script	82
B	Definition of thermal and mechanical parameters	87
B.1	Glass Transition Temperature	87
B.2	Young's modulus	87
B.3	Poisson's ratio	87

Chapter 1

Introduction

Throughout history, improving the performance of integrated circuits has been the primary focus. The request for better performance has led to transistors being made smaller and smaller and packing more transistors onto a single chip.

It is necessary to obtain higher speed and lower power dissipation.

For the speed, the RC delay, resistance and capacitance play a fundamental role. While to dissipate less power it is useful to decrease the parasitic capacitances. In both FEOL and BEOL device designs, reducing capacitance plays a key role in performance. To do this, studies have focused on the search for new dielectric materials with the aim of reducing capacitances but with solutions that guarantee the same yield and reliability while ensuring that sufficient mechanical, chemical, structural properties and low costs are maintained in the manufacturing processes.

As expressed in 2022IRDS_ES in Grand Challenges In the Near-term: beyond 2022 a transition from FinFET to gate-all-around (GAA) will start and, at the level of interconnections, the introduction of new materials with low relative electric permittivity which guarantees good heat dissipation represents the most important challenge. [1]

It is also reported that there are slowdowns in the reduction of the κ -value for the ILD layer due to mechanical strength, adhesion and manufacturability problems. The poor mechanical strength and adhesion properties of low- κ materials are obstructing their incorporation.

For this reason, the study of the GAAFET Vertical nanosheet technology is of interest, in particular, the FEOL structure has been analyzed. In the search for low- κ materials that could replace the classic dielectrics, the study of low- κ polymeric materials was undertaken. And the behavior as a spacer material in transistors was investigated.

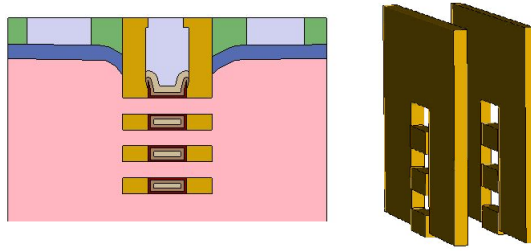


Figure 1.1. Spacer and inner spacer in GAAFET

This chapter introduces materials with low dielectric constant, an analysis of the dielectric constant spectrum in relation to various phenomena, and methods for reducing the value of κ .

In chapter 2, the fabrication process of V-stacked nanosheet GAAFET is reported, focusing on the dielectric of spacer and inner spacer.

In chapter 3, a dielectric polymer, polytetrafluoroethylene, which has a low value of κ , about 2.5, is analyzed with atomistic simulations, using QuantumATK. There are simulations of some electrical, mechanical and thermal properties.

In chapter 4, the NS-GAAFET device is simulated using Sentaurus. The electrical properties for the different spacer materials are analysed.

Finally, an analysis of future simulations to be done to better characterize the dielectric polymer and the behavior analyzes of the NS-GAAFET device.

1.1 Dielectric material and dielectric constant

An electrical insulating material with a resistivity greater than $10^9 \Omega m$ is considered a dielectric. The dielectric constant, κ , is a physical measure of the electric polarizability of a material.[5] [24]

Electric polarizability is the tendency of a material to allow an externally applied electric field to induce electric dipoles.

A dielectric material usually consists of electrically neutral molecules, each molecule or volume element can have a positive and negative charge separation. This charge separation is called electric dipole. Dipole charge separation generates a dipole electric field.

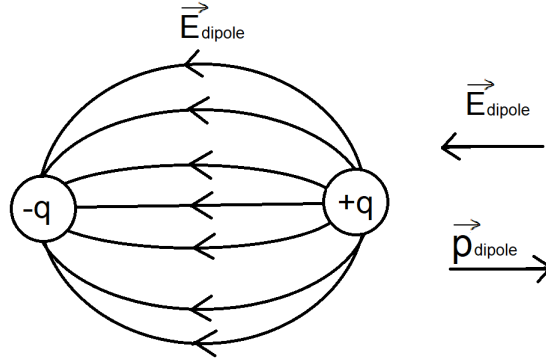


Figure 1.2. Field lines of the electric dipole

Choosing the barycenter of the charge $-q$ as pole, the electric dipole moment is:

$$\mathbf{p} = q \cdot \mathbf{r} \quad (1.1)$$

where \mathbf{r} is the position vector of the charge $+q$ with respect to $-q$.

Polarization \mathbf{P} is defined as the density of atomic electric dipole per unit volume [24]

$$\mathbf{P} = \frac{\sum \mathbf{p}}{V} = N\mathbf{p} \quad (1.2)$$

where \mathbf{p} is the dipole moment and N is the density of dipoles.

Let's analyze the relation between the different quantities in the polarization \mathbf{P} and displacement \mathbf{D} formulas with an external electric field \mathbf{E} .

$$\mathbf{D} = \epsilon_o \mathbf{E} + \mathbf{P} \quad (1.3)$$

\mathbf{P} is related to \mathbf{E} through χ_e the electric susceptibility of the dielectric.

$$\mathbf{P} = \epsilon_o \chi_e \mathbf{E} \quad (1.4)$$

Therefore

$$\mathbf{D} = \epsilon_o (1 + \chi_e) \mathbf{E} = \epsilon_o \kappa \mathbf{E} \quad (1.5)$$

where ϵ_o is the permittivity of the free space and κ the dielectric constant.

Dielectric constant κ also called relative permittivity ϵ_r .

$$\kappa = \frac{\epsilon}{\epsilon_o} \quad (1.6)$$

There are different polarization mechanisms:

1. **Electronic polarization.** It occurs in all solids, in neutral atoms, when an electric field displaces the nucleus relative to the surrounding electrons.



Figure 1.3. Electronic polarization

2. **Atomic or ionic polarization.** It occurs when adjacent positive and negative ions stretch under an applied electric field. The applied electric field distorts the arrangement of atomic nuclei within a molecule. Therefore, it is made possible by the elasticity of chemical bonds.



Figure 1.4. Atomic or ionic polarization

3. **Dipolar or orientational polarization.** It occurs in materials made up of polar molecules. The related dipoles can change their spatial orientation and tend to align according to the applied electric field.

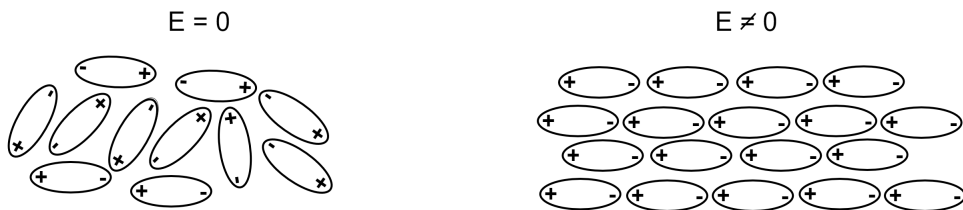


Figure 1.5. Dipolar or orientational polarization

4. **Interfacial polarization** It occurs when there is an accumulation of charge at an interface between two materials or between two regions within a material because of an external field.

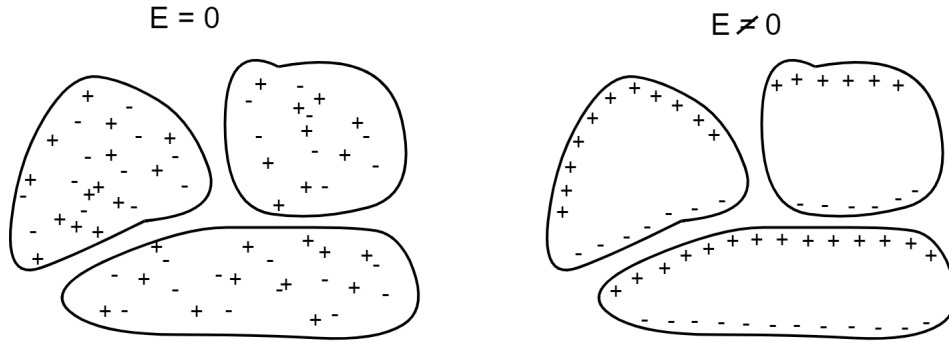


Figure 1.6. Interfacial polarization

In the vacuum, there are no elements to polarize, making $\chi_e = 0$ and $\kappa = 1$. In general, normal materials have a response to external fields that is dependent on the frequency of the field. This behaviour is due to the fact that when an electric field is applied, the polarization of a material is not instantaneous. Furthermore, a real dielectric subjected to an electric field can be traversed internally by a weak electric current. There are two types of dielectric losses: dielectric relaxation losses and ohmic losses. The former is due to the relaxation of the dipoles of the material, following the application of the electric field. The latter is an expression of the motion, supported by the applied electric field, of mobile charges inside the material. [5]

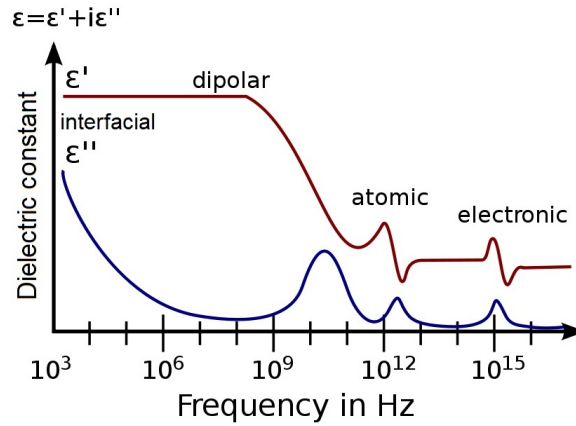


Figure 1.7. A spectrum of electric permittivity at different frequencies

Dielectric dispersion is the dependence of the permittivity of a dielectric material on the frequency of an applied electric field.

When the frequency becomes higher:

1. The dipolar polarization stops following the oscillations of the electric field at the frequency of 10^{10} Hz, the microwave region.
2. The atomic polarization and molecular distortion polarization fail to follow the electric field around the 10^{13} Hz, the infrared or far infrared region.
3. The electronic polarization follows the electric field up to around 10^{15} Hz, the ultraviolet region.
4. Interfacial polarization manifests itself from low frequencies up to a characteristic frequency, typical of the medium.

Polarization	$\tau[s]$	$f_{\tau}[Hz]$	band
Electronic	10^{-16}	10^{15}	UV
Atomic	$10^{-14} - 10^{-13}$	$10^{13} - 10^{12}$	IR
Dipolar	$10^{-11} - 10^{-3}$	$10^{10} - 10^2$	up to MW
Interfacial	$10^{-3} - 10^{-1}$	$10^2 - 10^0$	–

Table 1.1. Time constant and characteristic frequency for the different polarization mechanisms.

In the frequency region above ultraviolet, permittivity approaches the constant ϵ_o in every substance.

The atomic structure of dielectrics makes their dielectric strength relatively high, and therefore their use in capacitors is of interest.

By putting a dielectric in a capacitor the capacitance C of the latter is increased by a factor ϵ_r

$$C = \epsilon_r \epsilon_o \frac{A}{d} \quad (1.7)$$

where A is the area of the plates and d is the distance between the plates.

Static relative electrical permittivity, ϵ_r , can be measured by a practical method:

First, the capacitance of a capacitor, C_o , which has a vacuum between its plates, is measured.

Next with the same capacitor but with a dielectric between the plates the capacitance, C , is measured again. The relative permittivity is then calculated:

$$\epsilon_r = \frac{C}{C_o} \quad (1.8)$$

An important property of dielectric materials is the dielectric strength. This is the maximum electric field that under ideal conditions the dielectric can withstand before the avalanche breakdown process occurs and becomes electrically conductive. The avalanche breakdown process occurs in a few nanoseconds when the material is subjected to a very high electric field. The free electrons are accelerated and by collisions into atoms and molecules, they subsequently release other electrons, precisely creating an avalanche phenomenon. This creates an electrically conductive path and a powerful discharge passes through the material.

1.1.1 Low dielectric material

In the last decades, to limit the parasitic capacitances in integrated circuits there is a search for materials with low dielectric constant.

In fact, as can be seen from formula (1.7), the lower the dielectric constant, the lower the resulting capacitance.

Silicon dioxide is the most widely used dielectric material and its dielectric constant is between 3.9 and 4.2. Any material with a dielectric constant κ lower than 4.2 can be considered a low- κ dielectric. So low-k materials have a dielectric constant between 1 and 4.2. The minimum dielectric constant is 1 and it is the dielectric constant of the vacuum. Replacing silicon dioxide in integrated circuit manufacturing processes is very complicated. In fact, in addition to the κ value, there are many other properties that must meet the minimum requirements.[27]

Reduction of dielectric constant

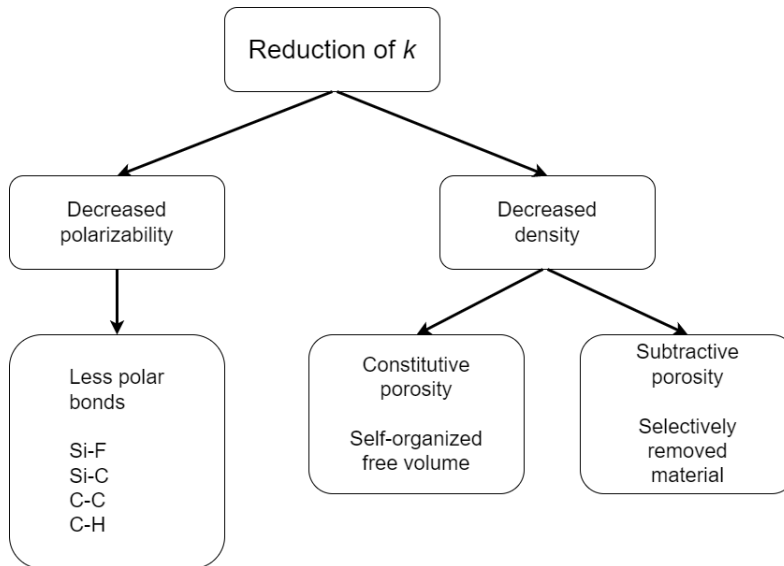


Figure 1.8. Possibilities for reducing the κ value of dielectrics.

As shown in the figure there are two ways to reduce κ : decrease the polarizability or decrease the dipole density. With the first method to obtain materials with low dielectric constant it is necessary that the chemical bonds are less polarizable than the Si-O bond. Instead the second method consists in a smaller number of dipoles. One method does not exclude the other and therefore they can both be used to obtain ultra low- κ materials.[27]

Over the years, attempts have been made to replace silicon dioxide with materials that have less polarizable bonds such as Si-C or Si-F. A further reduction was obtained with materials such as organic polymers which have non-polar bonds: C-C or C-H.

The low density of a material can be achieved in two ways: with materials that structurally have a lot of free volume or by creating pores in the material. In the first case we speak of constitutive porosity, in the second case of subtractive porosity.

Subtractive porosity is the method that lowers the dielectric constant the most because the pores can have a size of tens of nanometers and can reach a percentage of 90%.

The constitutive porosity is characterized by a percentage lower than 15% and also the size of the pores is relatively small, not exceeding 2 nanometres.

There is a classification of pores by size:

- micropores: smaller than 2 nm
- mesopores: between 2 and 50 nm
- macropores: larger than 50 nm

Subtractive porosity can be obtained by adding a substance called porogen which thermally degrades by exposure to UV rays or by selective etching. So after the degradation of this material, the pore is created.

This reduction of the dielectric constant can be mathematically described by Clausius-Mossotti. [3]

$$\frac{\kappa - 1}{\kappa + 2} = \frac{4\pi N}{3} \alpha \quad (1.9)$$

where κ the relative permittivity of the material, N is the number of molecules per unit volume (density), and α is the total polarizability, including electronic (α_e), distortion (α_d), and orientation (α_o) polarizabilities. To reduce the κ -value of a material, looking at the equation, one must decrease the density N and/or the total polarizability α . With a second equation it is possible to characterize the dielectric constant of a porous material. Let κ_1 be the dielectric constant of the material and κ_2 be the dielectric constant of the material inside the pore.

$$\frac{\kappa - 1}{\kappa + 2} = V \frac{\kappa_1 - 1}{\kappa_1 + 2} + (1 - V) \frac{\kappa_2 - 1}{\kappa_2 + 2} \quad (1.10)$$

where V is the average pore volume. If the material inside the pore is air, whose dielectric constant is approximately 1, the ratio to κ_1 in the equation equals 0. As a result, materials with low- κ and high porosity exhibit a very low resulting dielectric constant.[3]

Classification of low-k materials

There are different classification of low- κ materials.

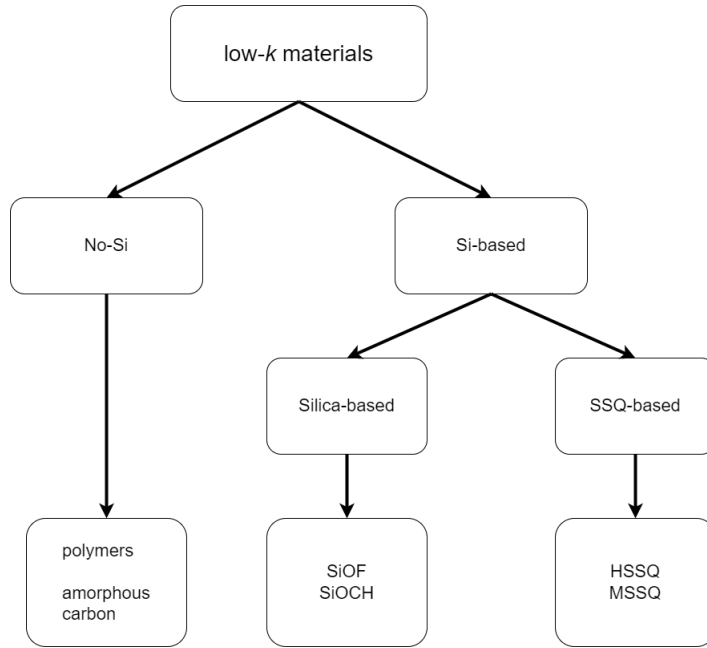


Figure 1.9. classification scheme of low- κ dielectrics.

As can be seen from the graph, low- κ materials can in the first instance be divided into silicon-containing and non-silicon-containing materials.

For materials containing silicon there are two viable ways as mentioned above. Lower the polarizability and therefore silica-based materials with the presence of F, C atoms or CH_3 groups.

Increase free volume and thus silsesquioxane (SSQ) based materials.

For silica-based materials, the addition of CH_3 further decreases the dielectric constant with more free volume.

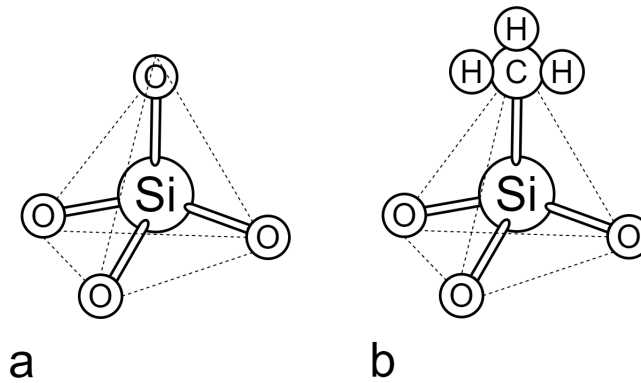


Figure 1.10. Representation of a tetrahedral silica unit (a) and the same unit of SiOCH material (b)

Silica has a tetrahedral structure while silsesquioxane materials have a cubic structure. Thanks to the cubic structure of the SSQ materials there is a low density and therefore a low- κ value.

Based on the termination of the cubic structures of SSQ there are two classifications: [27]

- HSSQ: SSQs ending in hydrogen atoms.
- MSSQ: SSQs ending with methyl groups (CH_2 and CH_3)

Oxygen atoms allow the different cubic structures to connect to each other. If subjected to high temperatures, the cubes can decompose and assume the tetrahedral structure of silica. Therefore both silica and silsesquioxane are often present and based on the percentage of this mixture the dielectric constant varies between 3 and 4. Dielectric constant which can be lowered with the introduction of pores.

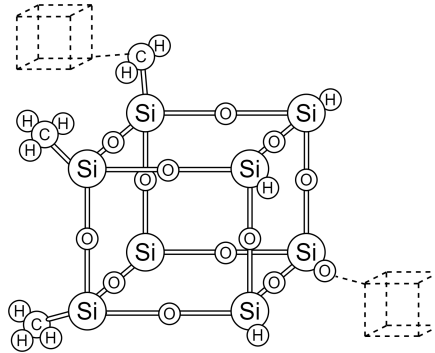


Figure 1.11. Representation of a silsesquioxane (SSQ) unit.

The main low- κ materials used that do not contain silicon are polymers. Polymers have the lowest dielectric constant values and for this reason they are of interest as a dielectric material for integrated circuits. The problem with these materials is that they have little mechanical and thermal stability and their compatibility in IC manufacturing processes becomes extremely difficult. Also for polymers the value of κ can be further decreased with porosity. Finally, there are materials such as zeolites or amorphous carbon but are currently of no interest.

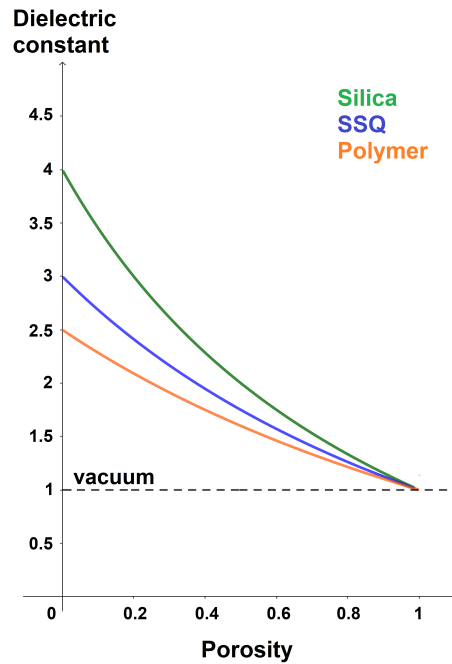


Figure 1.12. Dielectric constant as a function of porosity for different dielectrics.

As shown in the graph, as porosity increases, the dielectric constant decreases and polymers are the materials with the lowest dielectric constant value. Obviously, 100% porosity corresponds to vacuum for which the dielectric constant value is 1.

Another classification can also be made for porous low- κ materials. They can be divided into organics, inorganics and organic-inorganic hybrids.[29]

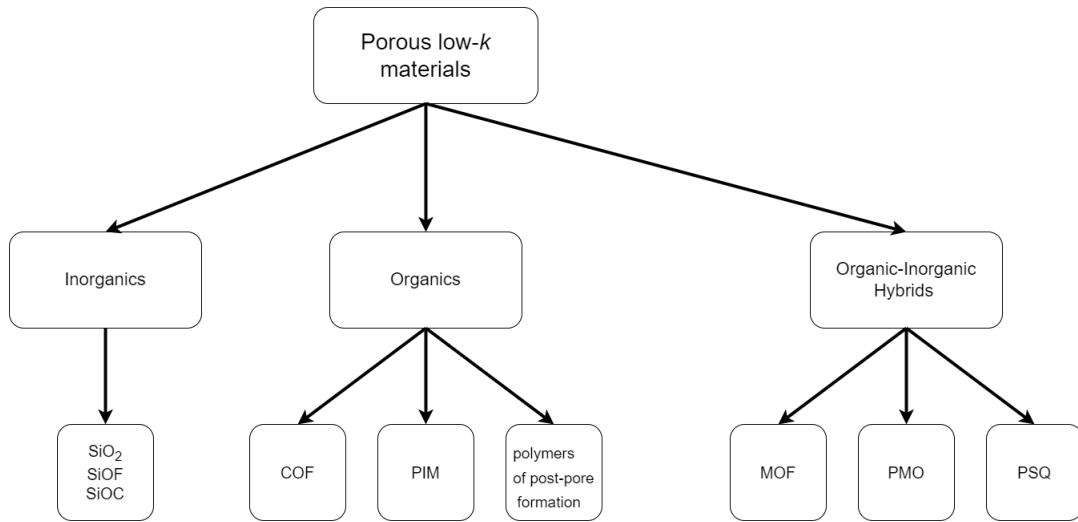


Figure 1.13. classification scheme of porous low- κ materials.

Generally, inorganic porous low- κ materials mainly include porous silicon dioxides (SiO_2), fluorine-doped silicon oxides (SiOF), and carbon doped silicon oxide (SiCOH).

Silicon dioxide has been and continues to be heavily used in semiconductor chips. In fact, SiO_2 has a number of qualities that make it the best material. It has a low dielectric constant, excellent mechanical and thermal stability properties and good compatibility with manufacturing processes. With porosity and air gap, it is possible to further reduce the value of κ .

As previously said, for the SiOF and SiCOH compounds, the less polarizable Si-F and Si-C bond is exploited with respect to the Si-O bond. This results in a decrease in the dielectric constant which can be further lowered with porosity.

Organic porous materials are so named because in addition to containing pores, they also contain organic elements such as C, O, H, N, B and others connected by covalent bonds.

Based on the formation of pores, they can be divided into three categories:

- covalent organic framework (COF)
- polymers of intrinsic microporosity (PIM)
- polymers of post-pore formation

Covalent organic frameworks are materials that have a low dielectric constant value that can even reach 1.2. They are characterized by small pores, usually less than 2nm, but recent studies have led to larger pores up to 4.7nm. To synthesize regular and periodic COFs we start from monomers with symmetrical structures and there are mainly two methods of synthesis: the co-condensation of aniline with aldehydes and the auto-condensation or co-condensation of boric acids. [29]

Intrinsic microporous polymers, whose name implies that pores are inherent in the polymer, are quite complex materials. They are complex both in terms of chemical structure and synthesis process. From this difficulty derives a difficult use in the semiconductor industry also having little chemical stability. Furthermore, intrinsic microporous polymers have small pores, but the dielectric constant can be decreased by increasing the free volume in the molecular structure. This is possible with the introduction of lateral groups which, being bulky, decrease the density. Furthermore, if this is not sufficient, fluorine atoms can be introduced which decrease the polarizability of the material.

Finally we have the polymers of post-pore formation so called because the pores are created after the formation of the material artificially.

There are two methods used: the template method and the etching method.

The template method is based on the presence of templates on whose surface the organic material is present. After formation the template is removed by chemical or physical processes. Subsequently, the removal of the template results in the pores being created.

The etching method is to form pores directly by creating free volume by removing some of the organic material. This removal is done through external stimuli such as heat or light.

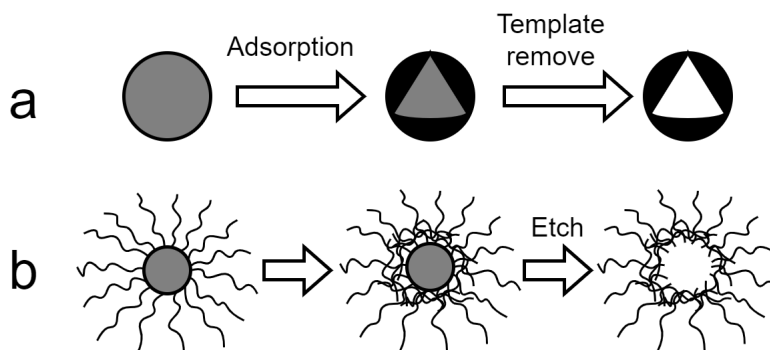


Figure 1.14. Representative preparations for polymers of post-pore formation: (a) template method, and (b) etching method.

These presented materials have advantages and disadvantages in terms of complexity, diffusion, economic aspect, thermal, chemical and mechanical stability and performance. To obtain the best properties of organic and inorganic compounds it was thought to synthesize organic-inorganic hybrid compounds.

These materials are of great interest as low- κ materials and the compounds used can be divided into three categories:

- metal-organic framework (MOF)
- periodic mesoporous organosilicon (PMO)
- polysilsesquioxane (PSQ)

Metal-organic frameworks (MOFs) are also known porous coordination polymers. They have this name because their structure is made up of metal nodes and organic linkers. They have an orderly, uniform structure with a high number of pores. They are synthesized according to the principle of coordination chemistry.

Due to the high porosity structure the dielectric constant is very low, but currently there are many practical problems of using MOFs because the mechanical stability and adhesion is not good during material making processes.

Periodic mesoporous organosilica (PMO) is synthesized by hydrolyzing and condensing bissilane precursors around a template. PMOs have pores whose size can vary greatly, between 2 and 50 nm.

This type of material presents a number of problems that currently hamper its implementation in practical fields.

Polysilsesquioxanes are prepared by hydrolysis of trifunctional siloxane monomers, which can be random, trapezoidal or cage structures, and usually adopt the chemical structure of $(\text{RSiO}_{1.5})_n$, where R is an organic group attached to each atom of Si, including hydrogen, alkyl, alkenyl, aryl and derivatives thereof. The good thermal stability of the materials is provided by the presence of Si-O. PSQs are characterized by good mechanical and thermal stability, have good corrosion resistance, hydrophobicity and other very good physical properties. For these reasons, it has been widely used in coatings, optoelectronic materials and other fields.

Ultimately, most of these materials have a very low dielectric constant value but present several problems in integrating current electronic production processes.

Integration of low- κ materials

A key step is the integration of low- κ dielectrics into integrated circuit manufacturing processes. Compared with silicon dioxide these low- κ materials are thermally and mechanically unstable, less compatible with other materials, absorb more water and chemicals and other problems. The main requirements that a low- κ material must possess are:

- Mechanical stability
- Thermal stability
- Hydrophobicity
- Chemical and physical stability
- Compatibility with other materials

An other important aspect for all functional materials is reliability in the user environment.

Mechanical stability During the integrated circuit manufacturing process, low- κ dielectric materials are subjected to heavy mechanical stresses that compromise their physical

integration. A quantity that determines mechanical stability is Young’s modulus. Mechanical stability decreases rapidly with increasing porosity. In fact, the Young’s modulus of SiO₂ is 76 GPa which becomes a few GPa when the porosity exceeds 50%. This relationship between elasticity and porosity is reported by the Phani and Niyogi equation.[8]

$$E = E_0 \cdot \left(1 - \frac{p}{p_c}\right)^f \quad (1.11)$$

Where E is the resulting Young’s modulus of the material, E₀ is the Young’s modulus of the poreless material, p is the percentage of porosity, p_c is the percentage of porosity at which the Young’s modulus is zero and f is a value which depends on the geometry of the pores of the material and the morphology of the grains.

It follows that low-κ materials also have a low Young’s modulus. There is often a compromise between porosity and Young’s modulus and therefore between dielectric constant and mechanical stability.

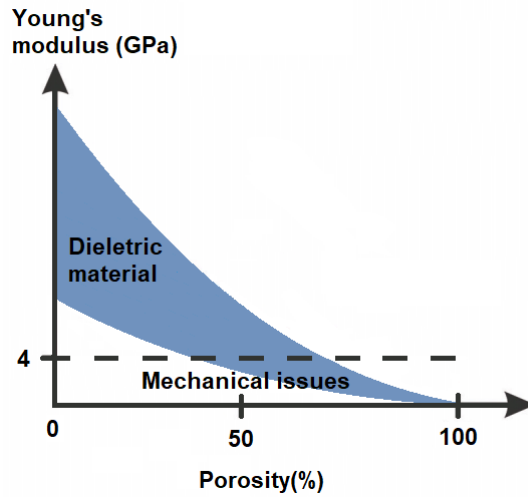


Figure 1.15. Young’s modulus of low-κ films as a function of porosity.

Thermal stability Another aspect that should not be underestimated is thermal stability. In manufacturing processes, temperatures can reach 400-450°C. Organic polymers, in particular, have a low glass transition temperature and numerous problems arise when this temperature is exceeded. Another example where it is important not to reach high temperatures is SSQ materials. As the temperature increases, SSQs increase their dielectric constant because the cubic structure decays into the tetrahedral one of silica.

Hydrophobicity Water is the main enemy of low-κ materials. Water has a κ value of about 80. It follows that the O-H bond is extremely polar. To prevent the low-k material from absorbing water, it must therefore be hydrophobic because a small amount would significantly increase the dielectric constant value. A big problem if you consider

that the air has an average humidity of 40-60%. For porous materials, the presence of pores can facilitate the absorption of water.

Usually, the polymers that do not have oxygen are hydrophobic and in general the hydrophobicity can be obtained with the presence of Si-H or Si-CH₃ bonds.

Chemical and physical stability During the IC manufacturing processes there are very delicate phases such as etching and cleaning. These phases can modify the chemical structure of low- κ materials by breaking bonds such as those of Si-C, Si-F and Si-CH₃ and replacing them with more polarizable bonds such as Si-O. These processes must be regulated to avoid this phenomenon and the more porous the material, the more delicate these phases are.

Compatibility with other materials This is a very important and often difficult requirement to meet. There are several aspects of compatibility between two materials to take into consideration. A quantifiable aspect is certainly the coefficient of thermal expansion. Mechanical damage can occur if the low- κ material has a very different CTE value than the material it is in contact with.

In integrated circuits, compatibility issues are evident in BEOL where there are copper interconnects and the dielectric surrounding them. As Cu is highly diffusive there is a thin barrier film between Cu and dielectric.

A first problem can certainly be the different CTE between the copper and the dielectric this is particularly true if the dielectric is made up of organic polymers.

Another problem can be the deposition of the barrier layer since if the dielectric is porous, the barrier layer will not be homogeneous. A high porosity also represents a further facilitation of the diffusivity of copper, with the danger of short circuits or performance degradation caused by the presence of parasitic elements.

Reliability Low- κ materials suffer from many reliability problems and for this reason SiO₂ or Si₃N₄ is still very present in integrated circuits as a dielectric because they offer greater guarantees of reliability.

Another disadvantage of low- κ materials is the low thermal conductivity which represents a limit in BEOL where there is a need to dissipate a lot of heat. If proper dissipation does not occur, there are problems such as copper electromigration.

1.2 Polytetrafluoroethylene

Polymers thus represent the next step as dielectrics in the development of electronic devices.

A list of the main polymers exhibiting a low dielectric constant. [17]

Polymer	dielectric constant
Polyacetal, Poly(methylene oxide), POM	3
Poly(acrylonitrile), PAN	3.1
Poly(Bisphenol A carbonate), PC	3.1
Poly(1,4-butadiene), PBD	2.3
Poly(1-butene), PB-1	2.2
Poly(butyl methacrylate), PBMA	2.7
Poly(caprolactam), PA 6	4.0
Poly(caprolactone), PCL	2.9
Poly(2-chloro-p-xylylene)	2.8
Poly(2-chlorostyrene)	2.8
Poly(4-chlorostyrene)	2.8
Poly(chlorotrifluoroethylene)	2.6
Poly(cyclohexyl methacrylate), PCHMA	2.7
Poly(2,6-dimethyl-p-phenylene oxide), PPI	2.7
Poly(2,6-diphenyl-p-phenylene oxide)	2.8
Poly(ethyl methacrylate), PEMA	2.9
Poly(ethylene terephthalate), PET	3.5
Poly(ethylene), PE	2.2
Poly(isobutene)	2.2
Poly(isobutyl methacrylate)	2.7
Poly(isobutylethylene)	2.2
Poly(methyl methacrylate), PMMA	3.0
Poly(2-methylstyrene)	2.5
Poly(4-methylstyrene), PMS, PPMS	2.5
Poly(1,4-phenyl ether) , PPE	2.9
Poly(propylene glycol), PPG	2.5
Poly(propylene), PP	2.2
Poly(p-xylylene)	2.6
Poly(thio-1,4-phenylene), PPS	3.0
Poly(α -methylstyrene) , P α MS	2.5
Poly[(tetramethylene terephthalate), PBT	3.2
Poly[bis(4-chlorophenyl)sulfone]-alt-[bisphenol-A], PSU	3.1
Polyhexamethylene adipamide, PA 6,6	4.0
Polyhexamethylene sebacamide, PA 6,10	3.5
Polystyrene, PS	2.6
Polytetrafluoroethylene, Teflon, PTFE	2.0
Polytetrahydrofuran, PTMO	2.5
Poly(vinyl acetate), PVAc, PVA	3.2
Polyvinyl chloride, PVC	3.0
Polyvinyl fluoride, PVF	2.1
Polyvinylidene chloride, PVDC	2.9
Polyvinylidene fluorid, PVDF	2.0

Table 1.2. Dielectric constants of polymers

One polymer of particular interest is polytetrafluoroethylene, PTFE, as it has a low dielectric constant of about 2 and a simple chemical composition. The monomer constituting PTFE is tetrafluoroethylene. Tetrafluoroethylene consists of two carbon atoms and four fluorine atoms (C_2F_4). As previously mentioned, the presence of fluorine atoms causes the material to have a low- κ value.

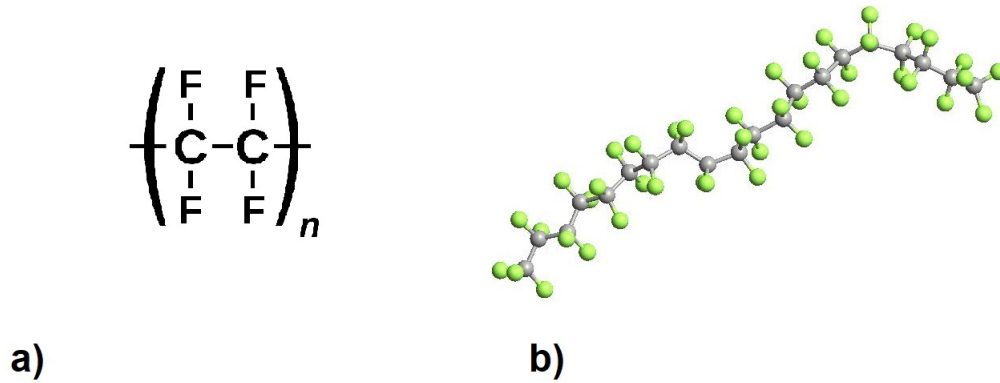


Figure 1.16. Chain of polytetrafluoroethylene

In figure a) the chemical formula of a PTFE chain and in figure b) a PTFE chain made up of 10 monomers.

The main properties of PTFE are summarized in the tables 1.3, 1.4, 1.5 and 1.6. [13]

Physical Properties	Metric
Density	2.00 - 2.30 g/cc
Water Absorption	0.000 - 0.0100 %

Table 1.3. Physical properties of PTFE

Mechanical Properties	Metric
Tensile Strength, Ultimate	13.0 - 55.0 MPa
Tensile Strength, Yield	20.0 - 196 MPa
Elongation at Break	70.0 - 600 %
Modulus of Elasticity	0.390 - 0.750 GPa
Flexural Modulus	0.275 - 0.700 GPa
Compressive Yield Strength	2.00 - 24.1 MPa
Poissons Ratio	0.460

Table 1.4. Mechanical properties of PTFE

Electrical Properties	Metric
Electrical Resistivity	1.00e+14 - 1.00e+19 ohm-cm
Surface Resistance	1.00e+15 - 1.00e+18 ohm
Dielectric Constant	2.00 - 2.10
Dielectric Strength	7.44 - 60.0 kV/mm
Dissipation Factor	0.000100 - 0.000200

Table 1.5. Electrical properties of PTFE

Thermal Properties	Metric
CTE, linear	75.0 - 790 $\mu\text{m}/\text{m}\cdot^\circ\text{C}$
Specific Heat Capacity	1.20 - 1.40 J/g $\cdot^\circ\text{C}$ @Temperature 40.0 - 260 $^\circ\text{C}$
Thermal Conductivity	0.167 - 0.300 W/m-K
Melting Point	321 - 344 $^\circ\text{C}$
Processing Temperature	379 - 429 $^\circ\text{C}$

Table 1.6. Thermal properties of PTFE

Part of these properties have been simulated through an atomic and process simulator QuantumATK.

Chapter 2

V-Stacked nanosheet GAAFET

GAAFET, Gate-all-around field effect transistor, is an innovative device that has allowed logic scaling to continue beyond 5nm technology.

Before GAAFETs, increasingly complicated challenges were faced to enable scaling. One above all the short channel effect (SCE). SCEs occur when the channel length is of the same order of magnitude as the source-drain depletion layers. High-k metal gate was another innovation that allowed for scaling.

FinFETs were the significant architectural change in the history of transistor devices to allow scaling by introducing trigate control. Below 7nm FinFETs have huge SCE problems and these problems are mitigated by GAAFETs.

In summary GAAFET provides very good gate controllability and therefore high immunity to short channel effects, thus allowing for maximum device scaling.

2.1 Fabrication processes

Most of the manufacturing processes of GAAFETs are compatible with that of FinFETs. In describing the process sequence, the starting point is a silicon substrate.[16]

2.1.1 Fabrication of Si-SiGe layers

The first step is the epitaxial growth of a Si-SiGe multilayer. The thickness of the layers varies between 7 and 12nm. SiGe has a typical percentage of germanium between 25 and 30%. For GAAFET with 3 nanosheets, there are 3 layers of Si and 3 layers of SiGe alternating between them.

Now the distribution of the layers is on the whole wafer and to define the channel width of the transistors the SIT (Sidewall Image Transfer) technique is adopted.

- a) It is therefore possible to proceed with the deposition of SiO_2 , Si_3N_4 and Si , called Buffer Oxide, Transfer Layer and Mandrel Layer respectively.

- **b)** The mandrel layer is modeled by mask etching into strips. Silicon dioxide spacers are created around these strips.
- **c)** The mandrel layer is etched as well as the underlying silicon nitride layer. So there remain fins of silicon dioxide and silicon nitride.
- **d)** The exposed oxide buffer is removed and the exposed Si-SiGe layers are etched. For the creation of the STI the etched region is filled with SiO₂ and then the CMP process.

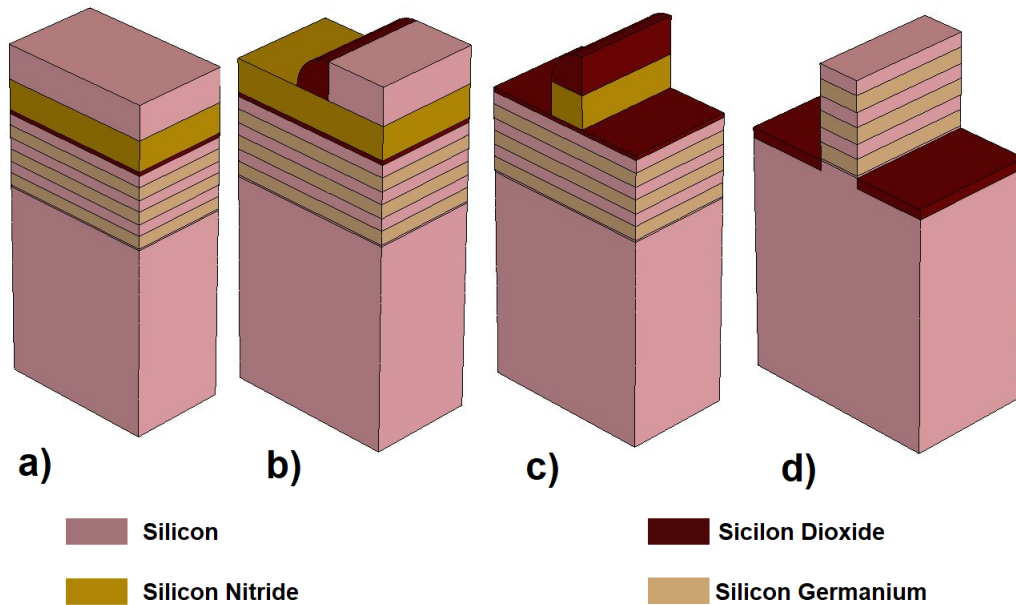


Figure 2.1. Fabrication of Si-SiGe layers

2.1.2 Dummy gate

Before the creation of the dummy gate,

- **a)** the TEOS is deposited and the subsequent CMP process. There is then a thermal oxidation process with a layer of silicon dioxide forming over the entire structure.
- **b)** At this point the dummy gate is created with polysilicon deposition and subsequent RIE process. With the modeling of the dummy gate it follows that the length of the channel is defined. The walls of the dummy gate are covered by a thin layer of oxide and the lightly doped source and drain regions are implanted (S/D extensions).

Phosphorus is implanted in the case of n-type GAAFET, while boron is implanted in the case of p-type GAAFET. A rapid thermal annealing process follows to activate the doping.

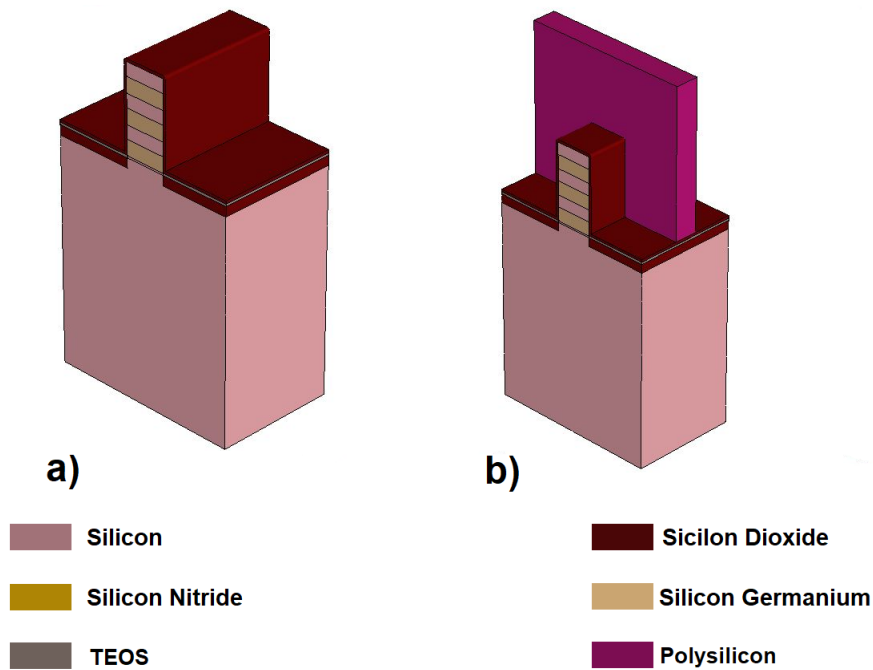


Figure 2.2. Fabrication of dummy gate

2.1.3 Spacer and inner spacer formation

At this point the manufacturing process of the spacer and inner spacer takes place. The classic material adopted is Si_3N_4 because it offers excellent mechanical and thermal properties.

- a) Deposition of silicon nitride and then anisotropic etching and isotropic overetching.
- b) Silicon carbon nitride is deposited and used as a hard mask to remove the oxide in the lateral regions of the gate.
- c) The exposed Si-SiGe layers are removed with anisotropic etching and subsequently partial SiGe etching takes place. The cavities are filled with silicon nitride and therefore the inner spacer is formed.

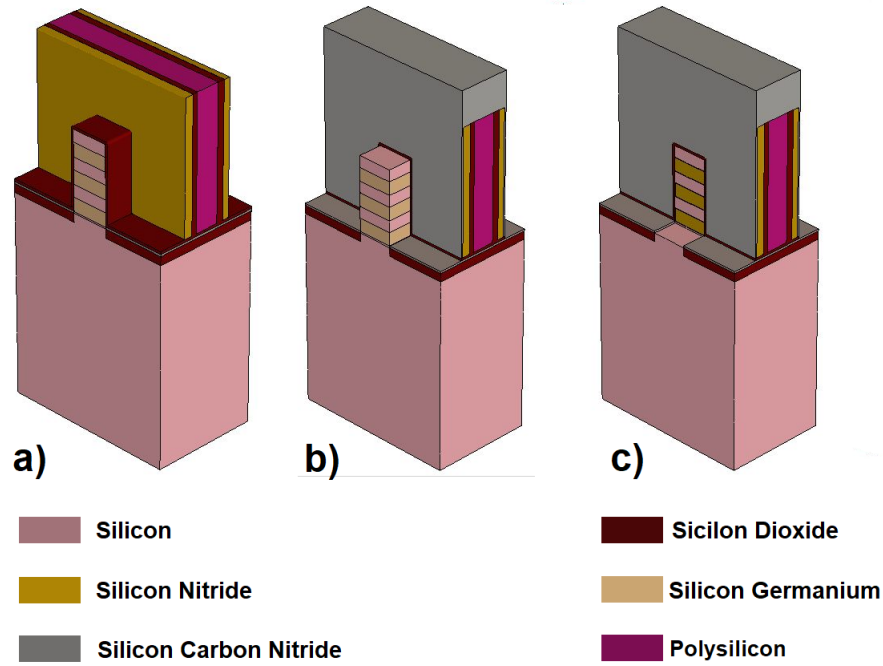


Figure 2.3. Fabrication of spacer and inner spacer

2.1.4 S/D epitaxial growth

For the formation of the source and drain regions,

- **a)** the epitaxial growth process of n- or p-type doped silicon is carried out depending on the type of GAAFET. To increase the mobility of the carriers, instead of silicon, silicon carbide can be used for the n-type GAAFET and silicon germanium for the p-type GAAFET.

To reduce the contact resistance S/D the silicidation process is used. Before the silicidation, SiCN is etched.

- **b)** The structure is covered with titanium and the titanium reacts with the silicon creating a layer of TiSi_2 . The excess titanium is then removed.

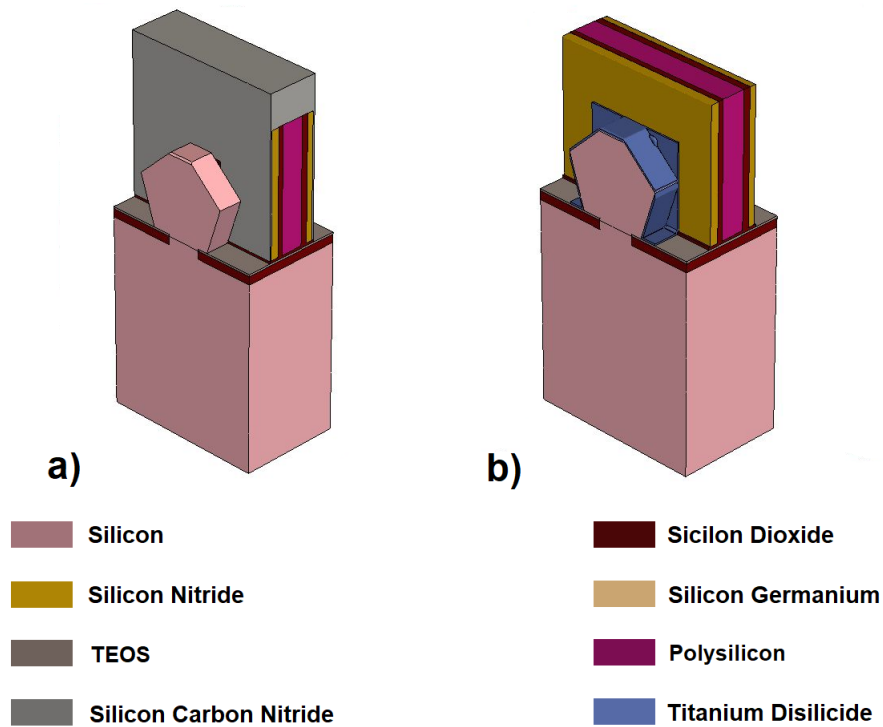


Figure 2.4. S/D epitaxial growth

2.1.5 Gate stack

Before the creation of the gate stack, the deposition of PSG takes place on the entire structure and the subsequent CMP process.

- **a)** Then the removal of the dummy gate with SiO_2 as the ESL and the removal of what is left of the SiGe layers.
- **b)** At this point we have the creation of the gate oxide consisting of a thin layer of silicon oxide which has a good interface with the silicon and then a thicker layer of high- κ dielectric such as hafnium dioxide.

The metal gate is made using metal-interdiffusion technology. There is a deposition of different layers of materials and the configuration changes between n-type and p-type GAAFET.

- **c)** For the n-type there are three layer of conductive materials: titanium nitride, tantalum nitride and titanium aluminide.

For the p-type there is an additional layer of titanium nitride between the tantalum nitride and the titanium aluminide.

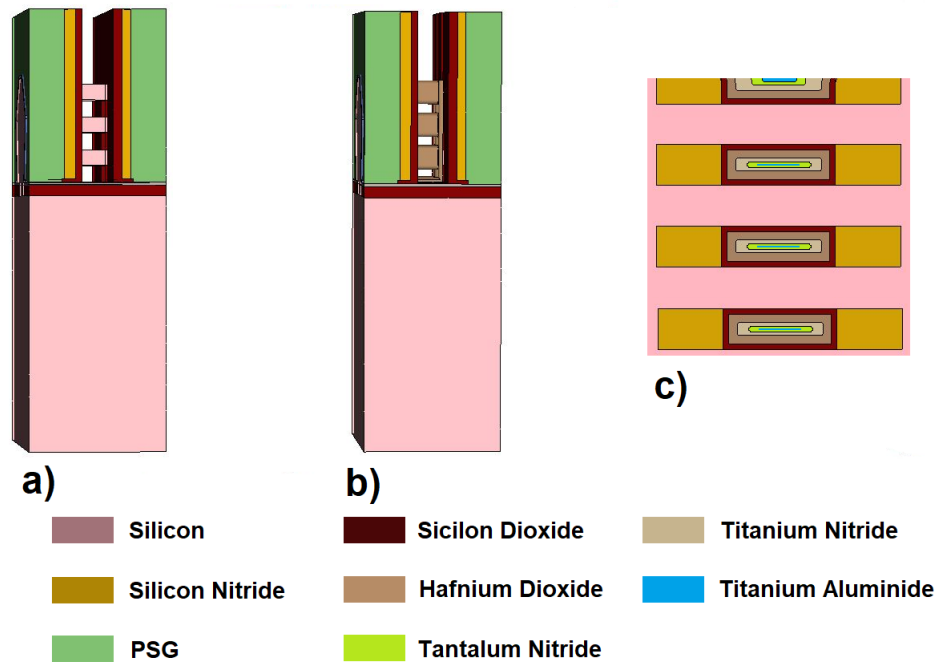


Figure 2.5. Fabrication of gate

2.1.6 Contacts

As the last step of the BEOL the gate, source and drain contacts are made.

- **a)** The gate is filled with tungsten and then the CMP process. A layer of silicon nitride is deposited on top of the gate.
- **b)** The contacts are made using the SAC technique. The cavities are made in correspondence with the source, drain and gate regions and tungsten is deposited until the cavity is filled.

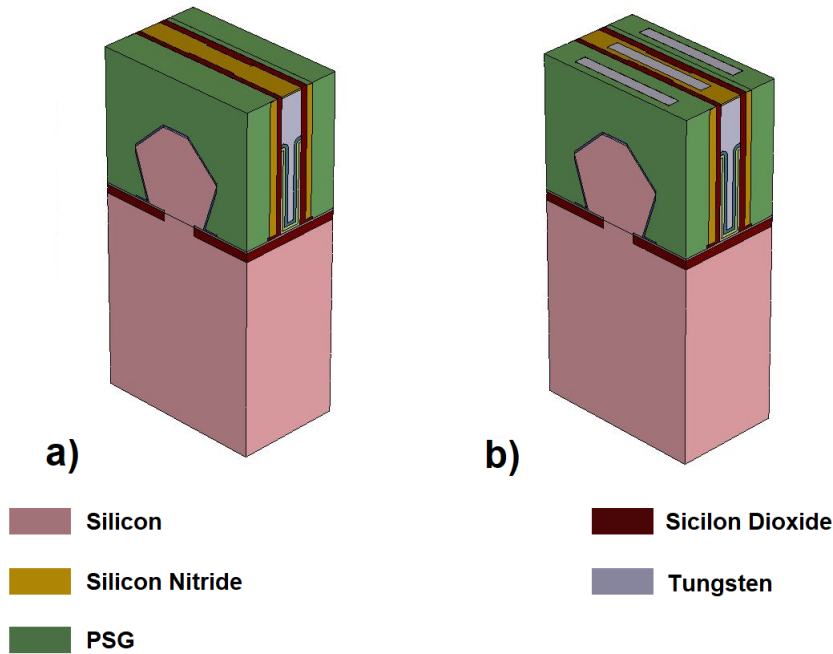


Figure 2.6. Fabrication of contacts

2.2 Inner spacer

The creation of spacers and inner spacers is a crucial step in the fabrication of transistors. The spacer is made to allow for less doped source and drain regions (low doped drain). Not having this LDD region near the drain, there would be a high electric field. [12] Carriers, electrons in the case of n-type transistors, in the channel subjected to a high electric field can collapse into the gate oxide. This phenomenon, which takes the name of hot electrons, in addition to damaging the gate oxide also leads to an accumulation of charge in the gate oxide and therefore to a translation of the threshold voltage V_{TH} . This problem concerns only the drain, but since the structure is symmetrical and the drain region is not known a priori, the LDD is implemented in both the source and drain regions.

Even more crucial is the creation of the inner spacer. In fact, there is the partial etching of the SiGe in the multilayer made up of Si-SiGe and the filling with the dielectric material. This process is on the scale of a few nanometers and the inner spacers are essential in order not to create short circuits between the gate and source and drain. [10]

Thus there is the gate and the source or drain spaced by a few nanometers with a dielectric material in the middle. It follows the importance of the perfect success of the manufacturing process of the inner spacers since an imperfect filling of the cavities would create a short circuit. Furthermore, the electrical properties of the dielectric material are also very important.

In addition to the electrical properties of the spacer dielectric, the mechanical properties are also fundamental. In fact, from this point of view, an important step in the manufacturing process of the transistor is the release of the channel, i.e. when the remaining SiGe of the multilayer is removed before the creation of the gate stack. In this phase, the whole spacer structure is subjected to strong mechanical stress and the nanosheets could collapse or misalign with failure in the realization of the transistor or performance degradation.

To guarantee good electrical insulating properties, the dielectric must have a low dielectric constant and high mechanical properties resulting, for example, in having a high Young's modulus value. Often, however, the two things do not get along, in fact, low- κ materials have poor mechanical and thermal properties. A compromise is therefore sought and this is the case of Si₃N₄ which, having a relatively high dielectric constant compared to silicon dioxide, has excellent mechanical and thermal properties. Si₃N₄ has a dielectric constant of about 7.3 against 3.9 of SiO₂, but has a maximum Young's modulus of almost 300GPa against 180GPa of SiO₂. It is also superior to SiO₂ in terms of thermal conductivity. [11]

Summarizing the manufacturing process of the inner spacers: after the recess of the epitaxial SiGe/Si lattice, a selective indentation of SiGe between the silicon NS is carried out, followed by inner spacer dielectric deposition and etch. Then SiGe is selectively removed (channel release) before high-K metal gate formation.

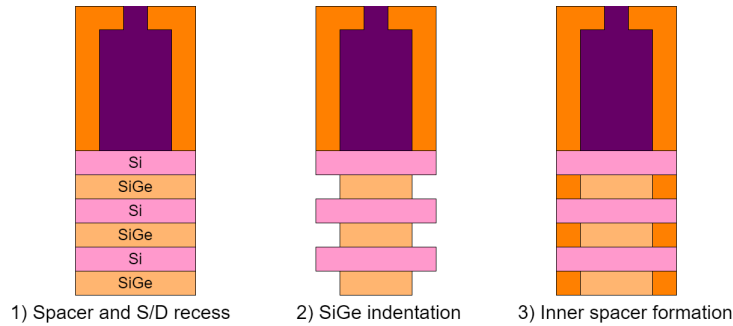


Figure 2.7. Inner spacer formation

Both for the creation of the inner spacer and for the release of the channel, the etching process must be very selective. It requires high etch selectivity of SiGe to Si and to exposed dielectrics. High selectivity in channel release avoids channel erosion and performance degradation.

The indentation process of the SiGe is fundamental for the definition of the characteristics of the device. The depth of the inner spacer and the silicon loss which determine the channel length L_g , the overlap of the transistor junction and the extension regions depend on it.

The thickness of the extended region therefore depends on the thickness of the inner spacer. The thickness of the extended region affects R_{on} . The thicker the extended region, the higher the R_{on} value. Furthermore, the thickness of the inner spacer also determines the

parasitic capacitance of the spacer. The greater the thickness of the inner spacer, the lower the parasitic capacitance. Consequently, there is a compromise on the thickness of the inner spacer and therefore its shape influences the AC performance. [23]

In the SiGe indentation process, the percentage of germanium for the same etching process determines the thickness of the cavity. The higher the percentage, the thicker the cavity. However, the higher the percentage of germanium, the higher the probability that it diffuses into the silicon. Usually the percentage of germanium is between 25 and 30%.

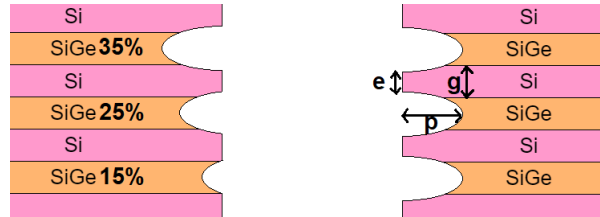


Figure 2.8. SiGe indentation process

The etching selectivity can be measured from the parameters in the figure.

$$etch\ selectivity = \frac{p}{|g - e|/2} \quad (2.1)$$

It is necessary that the selectivity is greater than 100:1 for a good manufacturing of the transistor.

2.3 Parasitic capacitance

There are several parasitic elements that characterize the GAAFET device. The figure shows the main parasitic resistances and parasitic capacitances that characterize the FEOL. [9] [7] [2]

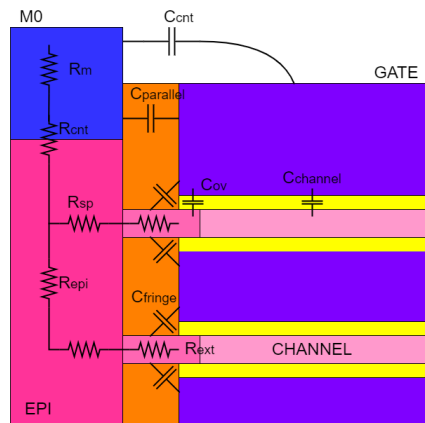


Figure 2.9. Parasitic elements in the GAAFET

The figure shows a section of the device in which the capacitances of the inner spacer are mainly analysed.

Other sections of the device would exhibit many other capacitances. In any case, the current figure shows some significant aspects that the spacer must have. First there is the channel capacitance, the capacitance between gate and channel that is the useful capacitance.

- C_{ov} is the overlap capacitance, the capacitance due to the S/D junction overlap under the gate.
- C_{cnt} is a capacitance due to two electrodes which are not parallel.

Parasitic capacitances involving the spacer are $C_{parallel}$ and C_{fringe} .

- $C_{parallel}$ is the resulting capacitance of parallel plates between gate and S/D epi or S/D contacts.
- C_{fringe} is the capacitance between the gate sidewall and the S/D junction through the spacer.

Therefore, in order to reduce these last two parasitic capacitances, the spacer must have a low relative permittivity value and the thickness of the spacer must be high.

As already mentioned, the condition on the thickness of the spacer also affects the length of the extended region and therefore increases R_{ext} .

Chapter 3

Atomistic simulations in QuantumATK

QuantumATK is an integrated platform of atomic-scale and electronic modeling tools written in Python and C++. [21]

Atomistic modeling allows detailed insight into processes with analysis at the atomic level leading to more efficient development through higher quality results.

Time and cost are reduced in the development of semiconductor technology using QuantumATK by enabling earlier optimization of material and transistor processes.

The use first of QuantumATK and then of Sentaurus allows a continuous flow from the analysis of materials and processes to the design of the devices.

The atomic-scale modeling tools in QuantumATK range from classical force fields for handling large and somewhat more realistic material systems to tools that provide highly accurate results for smaller systems.

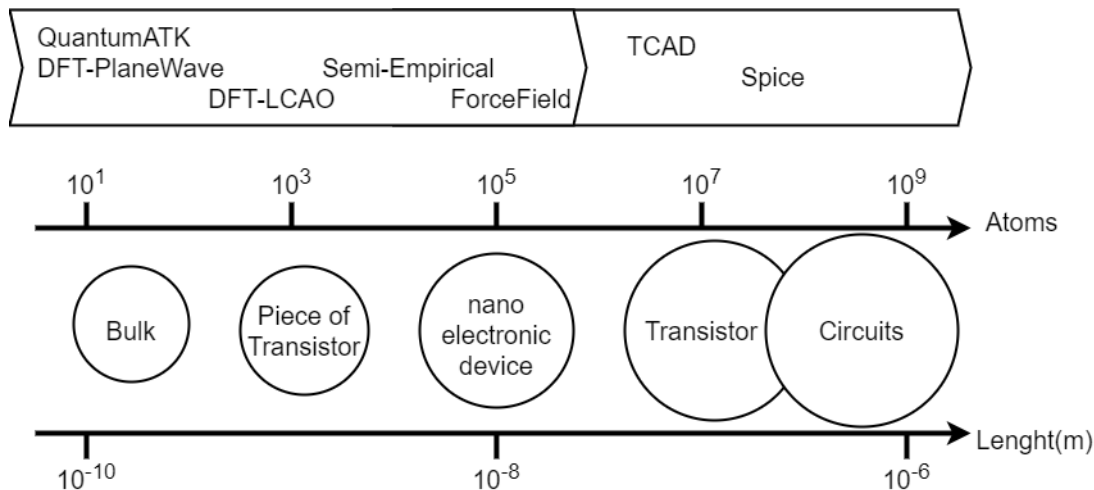


Figure 3.1. Design flow from QuantumATK to Sentaurus TCAD.

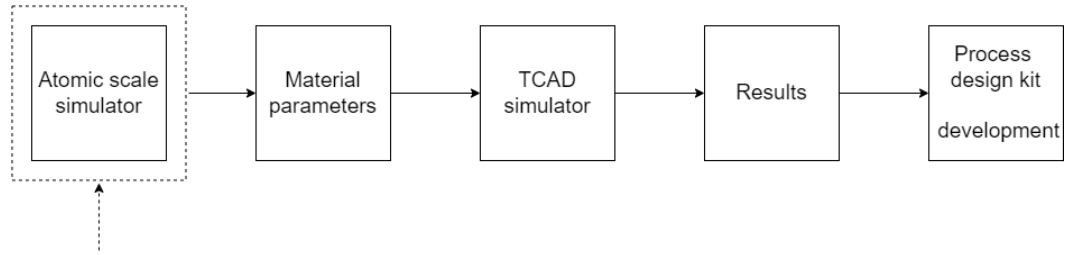


Figure 3.2. Design flow from atomic scale simulator to process design kit.

QuantumATK combines the effectiveness of Python scripting with the ease of use provided by a graphical user interface. All simulation engines share a common infrastructure for parallel analysis, ion dynamics, and performance techniques. The platform consists of the following components:

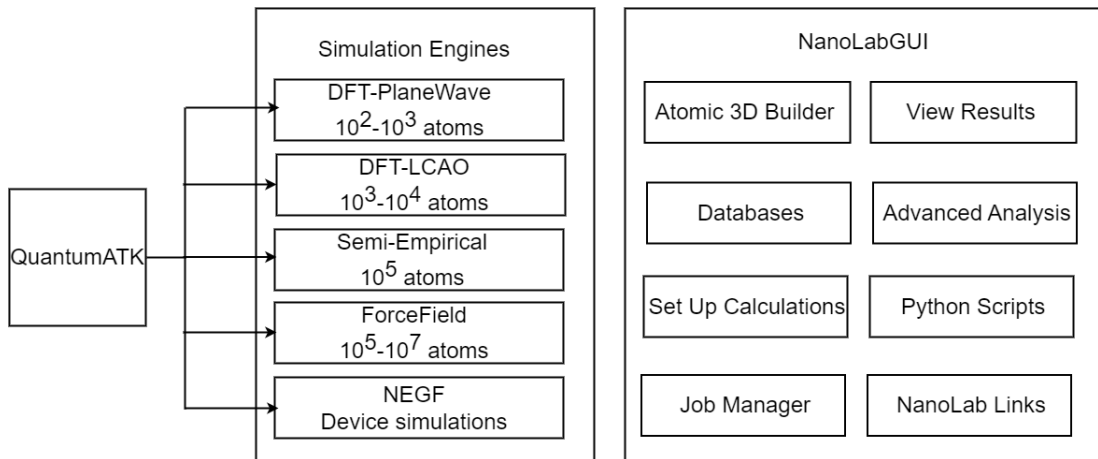


Figure 3.3. Structure of QuantumATK platform

Calculators

- **DFT-LCAO**: Simulation engine for density functional theory (DFT) using pseudo-potentials and linear combinations of atomic orbitals (LCAO) basis sets.
- **DFT-PlaneWave**: Simulation engine for DFT using pseudo-potentials and plane-wave basis sets.
- **SemiEmpirical**: Semi-empirical simulation engine using DFTB, extended Hückel, Slater-Koster, and other tight-binding models.
- **NEGF**: Module for nanoscale device and transport simulations using non-equilibrium Green's function (NEGF) methodology. Uses either DFT-LCAO or the SemiEmpirical module for describing the Hamiltonian of the system.

- **Surface Green's Function:** Module for modelling of surfaces beyond the slab approximation. Allows for treating electro-chemical reactions and surface states. Uses either DFT-LCAO or the SemiEmpirical module for describing the Hamiltonian of the system.
- **ForceField:** Simulation engine for atomic-scale simulations (e.g. molecular dynamics) using classical potentials such as bonded and reactive force fields, pair potentials, and other parameterized interaction models for atoms.

The recommended way to use QuantumATK is through NanoLab. It is a guide on the preparation phase allowing you not to get lost in the technical details but in modeling what you want to do thanks to the graphic help. NanoLab also offers important tools for data analysis. A typical workflow in NanoLab consists of the following steps:

1. Create atomistic structure
2. Set up simulations
3. Run a job
4. Analyze results

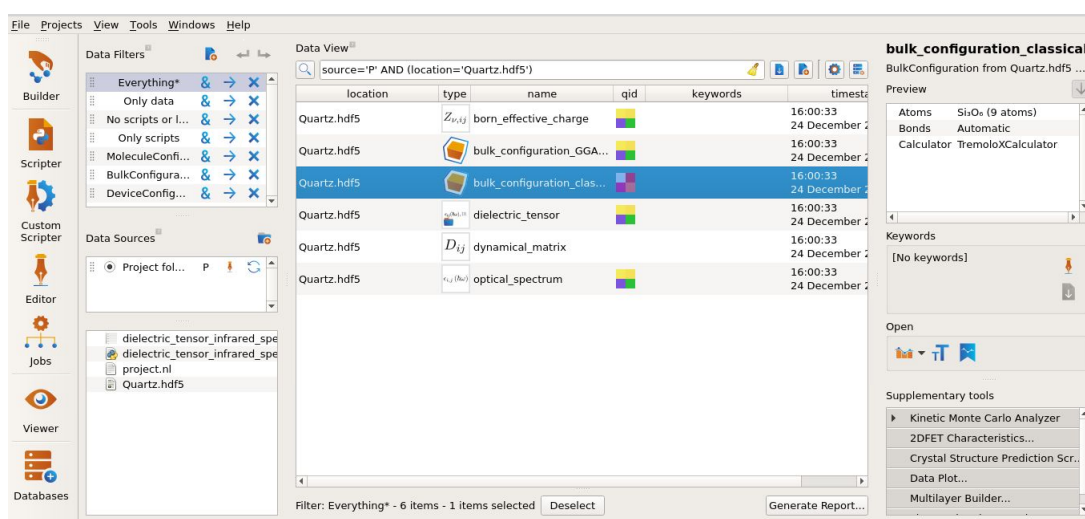


Figure 3.4. The QuantumATK GUI.

The QuantumATK graphical interface looks like the figure 3.4. On the left are the different tools:

The **Builder** is an essential part of the QuantumATK graphical user interface to the QuantumATK calculator engines. The Builder provides a range of powerful tools for building advanced atomic scale structures, e.g. bulk crystals, 1D nanowires, 2D nanosheets, clusters, and device configurations with either one or two probes. After a structure is built, it

can be used either in QuantumATK calculations or exported to external file formats for use in other atomic-scale simulation packages.

In the **Scripter** generator, you can create new objects called Workflows, automatically saved as .hdf5. A workflow consists of one or more components called Blocks. A block represents one or more calculation steps and it exposes calculation parameters. Calculation parameters can be edited from the Scripter generator. Creating a workflow is as easy as assembling blocks from a catalog of built-in blocks. You can export a workflow as a Python script.

In **Custom Scripter** you use the graphical user interface QuantumATK to set up your VASP calculations.

The **Editor** for viewing and editing Python scripts.

The **Job Manager** for local and remote execution of QuantumATK scripts. The Submission Settings widget has two basic panels:

- Job type
 - Serial
 - Threaded parallel (single process)
 - Multiprocess parallel
- Job properties
 - Threading
 - MPI Parallelism
 - Use separate temporary directory

The **Viewer** provides beautiful and easy to use 3D view and selection functionalities.

Databases, QuantumATK contains an internal database with several hundred crystals, molecules and fullerenes.

3.1 Polymer Builder

Polymer Builder is a tool introduced in QuantumATK Q-2019.12 for creating polymers using the Nanolab GUI. Polymer Builder is used to create a diverse variety of polymers from homopolymers to polymer blends, it is possible to include embedded molecules, nanoparticles and surfaces.

Once the initial model of the polymer has been created, it is possible to carry out various simulations of a mechanical, thermal and electrical nature. [20]

Different configurations of polytetrafluoroethylene have been made with the use of Polymer Builder.

3.1.1 Procedure of the Polymer Builder

To use polymer builder you need to perform the following steps:

1 Open the **Script Generator**.

2 Add the **Polymer Builder** block under the **Generator** into the templates. In the **Monomer Database**, there are several monomers of different polymeric sequences. You can create and upload new monomers to the **Monomer Database**.

Monomer Database	
name	group
1,1-Difluoroethylene	Vinyl Monomers
2-Butene	Vinyl Monomers
Adipic Acid	Condensation Monomers
Cis Butadiene	Vinyl Monomers
Ethylene	Vinyl Monomers
Ethylene Glycol	Condensation Monomers
Ethylene Glycol Peo	Condensation Monomers
Ethylenediamine	Condensation Monomers
Hexamethylenediamine	Condensation Monomers
Hydroxystyrene	Vinyl Monomers
Methyl Acrylate	Vinyl Monomers
Methyl Methacrylate	Vinyl Monomers
Propylene	Vinyl Monomers
Styrene	Vinyl Monomers
Terephthalic Acid Amide	Condensation Monomers
Terephthalic Acid Ester	Condensation Monomers
Tert Butoxycarbonyloxystyrene	Vinyl Monomers
Tert Butyl Methacrylate	Vinyl Monomers
Tetrafluoroethylene	Vinyl Monomers
Trans Butadiene	Vinyl Monomers
Vinyl Butadiene	Vinyl Monomers
Vinyl Chloride	Vinyl Monomers

Table 3.1. Monomer database QuantumATK

There are 5 sections for entering data to obtain the desired polymer. They are Polymer Sequence, Polymer Environment, Pre-equilibration, Force Field and IO.

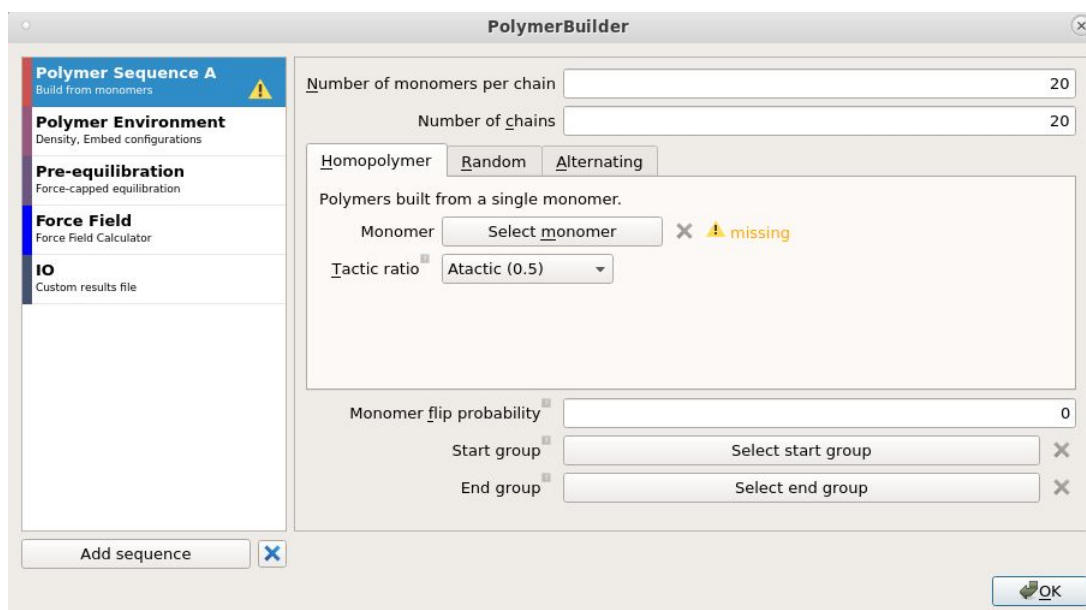


Figure 3.5. Polymer Builder in the Script Generator

3 Create the polymer sequences. In polymer sequence A, the different type of polymer sequence is selectable: Homopolymers, Random and Alternating. With homopolymer there is only one type of monomer making up the polymer chain, with random there are more monomers making up the chain in a random order and finally with alternating the different monomers alternate in a pre-established order.

You can choose the number of monomers per chain and the number of chains.

Tactic ratio is a value between 0 and 1 and determines how biased the selection of monomers is toward the same (0) or alternating (1) monomer addition points, for monomers with two stereochemical substitution groups. These are isotactic and syndiotactic polymers respectively. Atactic random polymers are specified with 0.5, which shows no bias towards either addition point.

You can also add the different polymer sequences by clicking the button of Add Sequence. In the construction of polytetrafluoroethylene, tetrafluoroethylene is selected as monomer and the number of monomers and chains were varied in the different simulations.

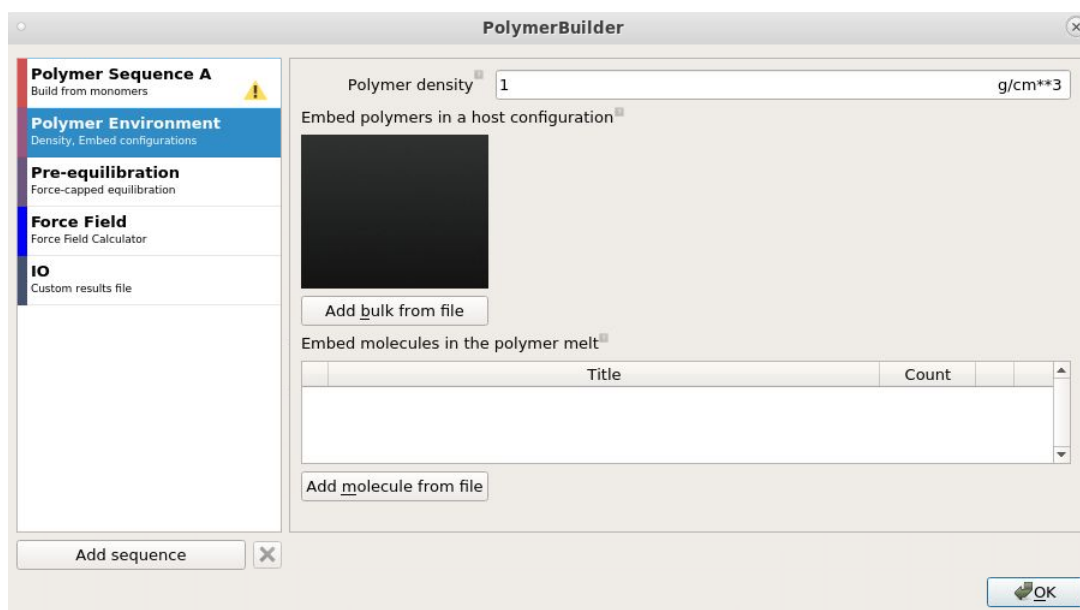


Figure 3.6. Polymer Environment in the Script Generator

4 In the Polymer Environment, the density of the polymer can be set and it is possible to incorporate molecules, nanoparticles or surfaces into the polymer. A molten polymer is created whose density is controlled by the size of a periodic box. In the case of embedded particles, the polymers are packed in the periodic box of the host configuration. You can choose to create polymers with different embedded material types.

For PTFE the polymer density is set to 2.2. The density can also be changed later from the builder section by moving the position of the chains and changing the size of the simulation box.

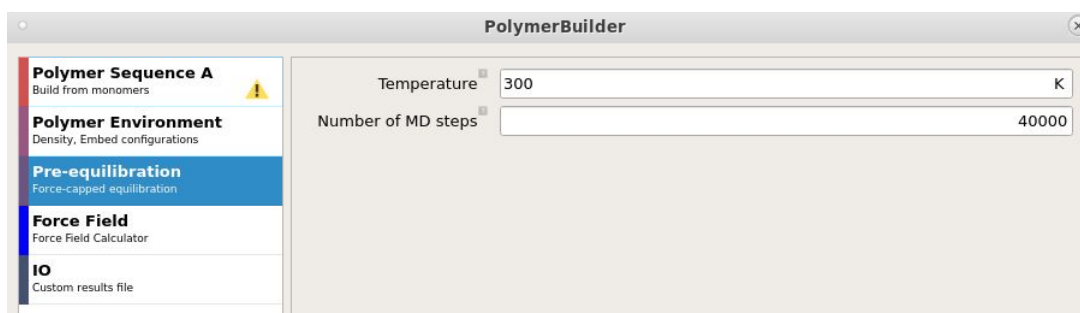


Figure 3.7. Pre-equilibration in the Script Generator

5 Next is the Pre-equilibration section. The initial model of the polymer is generated by means of Polymer Monte Carlo. Subsequently there is the pre-equilibration which serves

to avoid the overlapping of atoms or that they are too close through the use of the Force-capped equilibration method. In this section, you can choose the temperature at which the force-capped equilibration will be run and the number of MD steps that are run at each level of force capping.

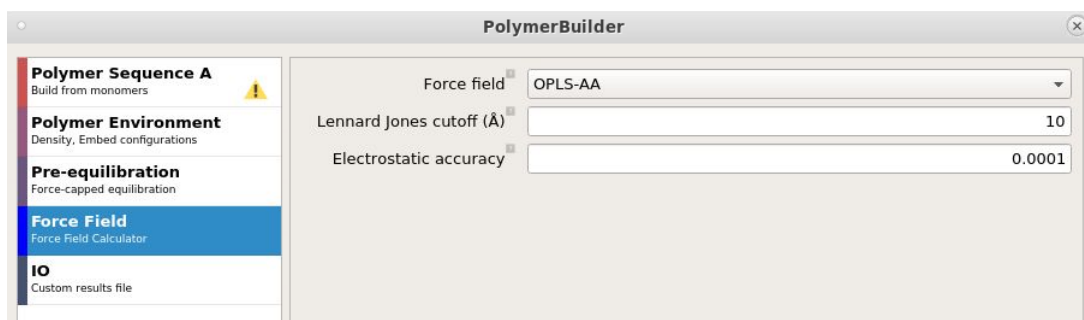


Figure 3.8. Force Field in the Script Generator

6 Polymer Builder includes the Dreiding or OPLS force field. The Dreiding force field is much simpler than OPLS force field. Polymer Builder can automatically indicate the types of Dreiding force field.

Using Dreiding force field automatically adds the tags of the atoms, but does not describe tacticity and partial charge. In contrast, OPLS force field considers the tacticity and partial charge of atom types. Ultimately OPLS is more complex but more accurate.

7 Run it using the **Job manager**. Usually a polymer is more complex than a molecular bulk system. There are more atoms, the size is larger and therefore the simulation times are longer. The pre-equilibration phase is particularly long.

Once the simulation is finished, it is possible to observe the results through the Viewer tool.

By selecting the .hdf5 file, two types of object appear that can be opened with the Viewer: one is the configuration after polymer Monte Carlo and is called BulkConfiguration_0 and the other is the configuration after the pre-equilibration process and is called BulkConfiguration_1.

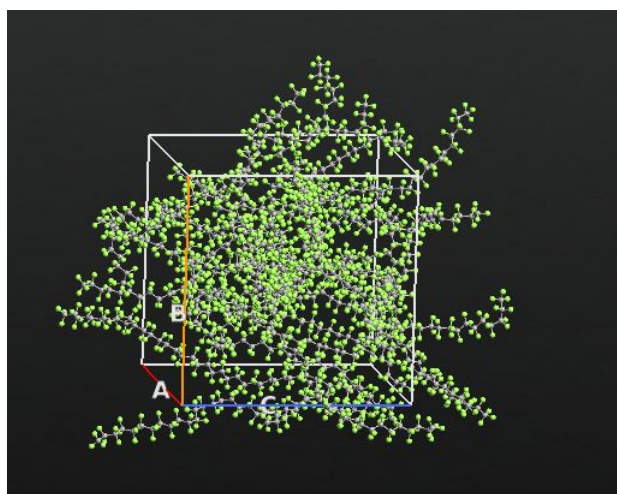


Figure 3.9. Example: 20 chains with 20 monomers per each chain of Polytetrafluoroethylene with $2.2g/cm^3$ density.

3.1.2 Analyzing the electrical properties of a polymer material

One of the most important electrical properties to analyze for a dielectric material is the dielectric constant. The analysis of the dielectric tensor was then carried out using a script with the calculator blocks shown in the figure. [19]

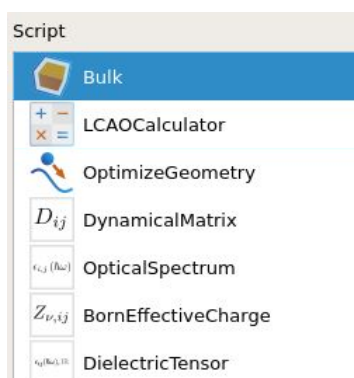


Figure 3.10. Script of the dielectric tensor simulation

There are many blocks and different parameters to set. The main changes to the default parameters are:

- LCAO Calculator
 - In Exchange correlation set family to GGA and set spin to unpolarized.
 - In Dispersion correction set Van der Waals correction to Grimme DFT-D3.

- In Functional Predefined set functionals to PBE.
- In Basis Sets set Pseudopotential to PseudoDojo and Basis Set to DoubleZetaPolarized.
- Optimize Geometry
 - Set Force tolerance to 0.001eV/Å.
 - Set Stress error tolerance to 0.1 Gpa.
 - Set maximum number of steps to 200.
 - Set maximum step size to 0.2Å.
- Dynamical Matrix
 - Set Repetitions to (1,1,1).
- Optical Spectrum
 - In Energy range set E_0 to 0 and E_1 to 0.17eV which corresponds to a frequency range from 0 to 40THz. Set points to 501.
 - In Parameters set Bands below Fermi level and Bands above Fermi level to 200.
 - In k-point Sampling set Preset densities to 7Å.

The Python script executed is reported in the appendix.

The dielectric response is calculated as the sum of the electronic part and the ionic part.

$$\epsilon_{r,\alpha\beta}(\omega) = \epsilon_{r,\alpha\beta}^{elec}(\omega) + \epsilon_{r,\alpha\beta}^{ionic}(\omega) \quad (3.1)$$

where ϵ_r is the relative permittivity and α and β are the Cartesian coordinate.

The electronic part is calculated from the **OpticalSpectrum** while the ionic part is calculated from **BornEffectiveCharge**.

At high frequency,

$$\epsilon_{r,\alpha\beta}^{\infty} = \epsilon_{r,\alpha\beta}^{elec}(0) \quad (3.2)$$

The simulations were carried out with different configurations of PTFE. Since the simulation time increases significantly as the number of atoms increases, the simulated configurations are:

- PTFE two monomers, single chain (PTFE_2_1)
- PTFE two monomers, two chains (PTFE_2_2)
- PTFE four monomers, four chains (PTFE_4_4)

Since the dielectric constant depends on the density, simulations were made with different density values.

PTFE_2_1 dielectric tensor

The first simulation has a polytetrafluoroethylene bulk configuration consisting of a single chain of two monomers (C_4F_{10}).

The density obtained by changing the size of the simulation box is 2.262 g/cm^3 .

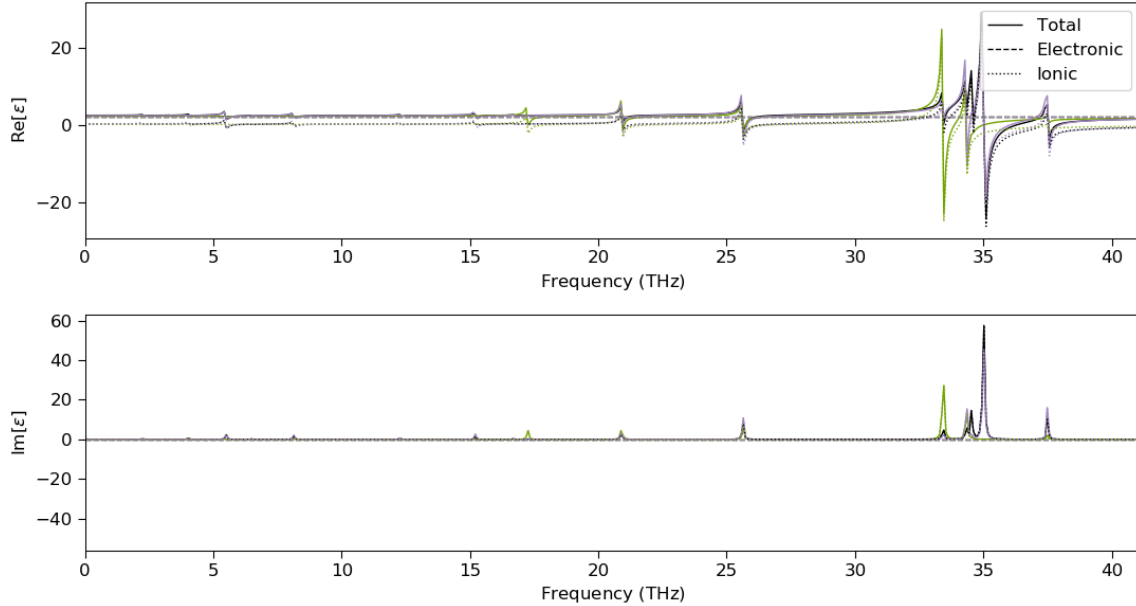


Figure 3.11. Dielectric constant of PTFE_2_1

This is the result of the simulation in which the graph of the dielectric constant versus the frequency is reported.

There are two graphs, one for the real part and one for the imaginary part. The frequency axis reaches a maximum value of 40 THz. There are high frequency peaks due to the phenomena described in chapter 1.

The graphs show the curve of the electronic part, the ionic part and the total curve. These three curves are calculated for the x, y and z directions. If the material is regular and symmetrical there are no differences in the dielectric constant based on the direction.

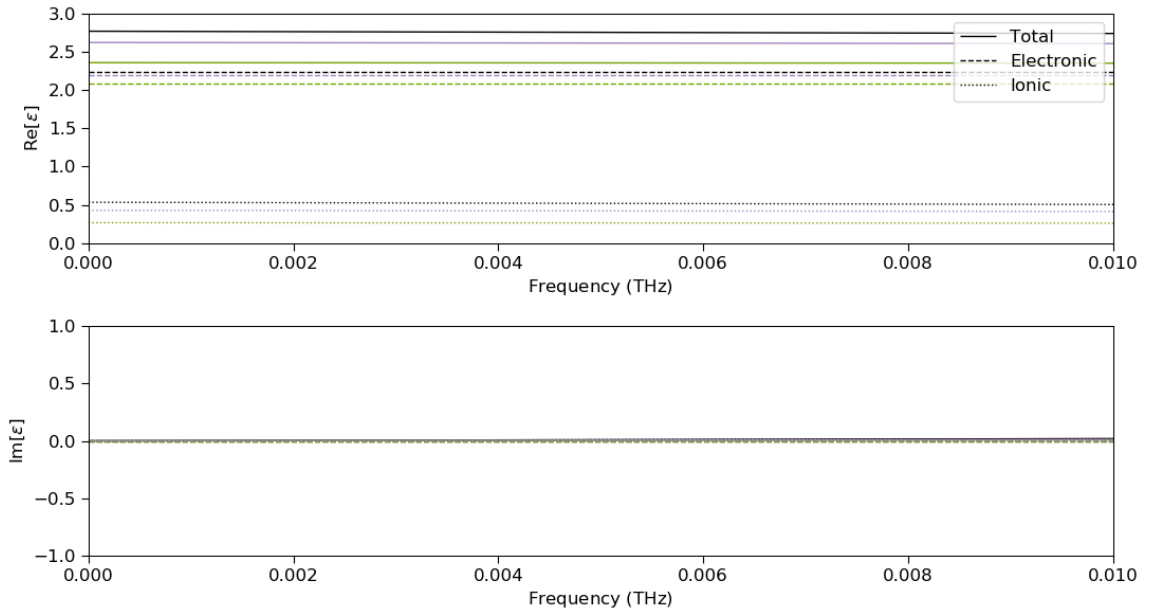


Figure 3.12. Dielectric constant of PTFE_2_1 at low frequency

Analyzing the dielectric constant at low frequency, several interesting aspects can be noted.

The imaginary part comes out as null and the real part has different results depending on the direction. The contribution of the ionic part is much lower than the electronic part and the maximum total value found is 2.76 and an average value of 2.58.

PTFE_2_2 dielectric tensor

The same simulation was performed by changing the bulk configuration of polytetrafluoroethylene. In particular, with a configuration composed of two chains having two monomers each. Furthermore, several simulations were carried out by changing the density.

In order to make a comparison with PTFE_2_1 let us first analyze the simulation of PTFE_2_2 with a density of 2.247 g/cm^3 . So slightly lower close density. Also in this case there are high frequency peaks of the dielectric constant and zero imaginary part at low frequency.

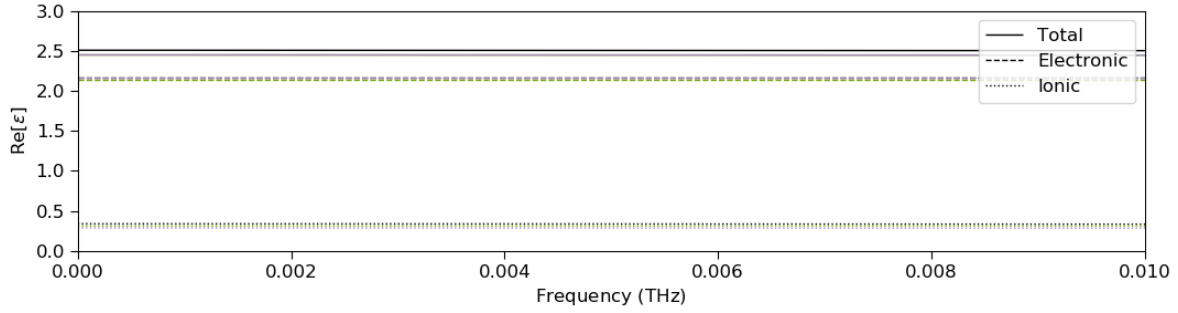


Figure 3.13. Real part of dielectric constant of PTFE_2_2 with density 2.2 g/cm^3 at low frequency

The first interesting thing is that in this case, the dependence on the direction is less evident and negligible with the lines that are almost overlapping.

Another very interesting thing is that the total value is 2.5, very close to the expected value and compatible with the total value of PTFE_2_1 as here the density is lower.

The simulations with different densities show very similar behaviour and the value of the dielectric constant changes.

PTFE_2_2	
density	dielectric constant
0.552 g/cm^3	1.33
1.193 g/cm^3	1.87
1.818 g/cm^3	2.21
2.247 g/cm^3	2.5

Table 3.2. PTFE_2_2 dielectric constant with different density

By prediction the value of the dielectric constant increases as the density increases.

PTFE_4_4 dielectric tensor

Finally, the configuration with 4 monomers per chain and 4 chains was simulated. This simulation was done to get a match with a more consistent number of atoms (104 atoms). Simulation times have become very long and for this reason it has not been possible to go further.

The density of the simulated PTFE is 2.213 g/cm^3 . At high frequency peaks similar to the previous simulations were found. At low frequency, the difference of the dielectric constant according to the direction is visible with a maximum value of 2.45 and an average value of 2.34.

Configuration	density	dielectric constant
PTFE_2_1	2.262 g/cm^3	2.58
PTFE_2_2	2.247 g/cm^3	2.5
PTFE_4_4	2.213 g/cm^3	2.34

Table 3.3. Comparison of the dielectric constant between the different configurations of PTFE with a density of 2.2 g/cm^3

Comparing the different configurations of PTFE with a density of 2.2, results are found which are compatible with slight differences due to slight differences in density.

3.1.3 Analyzing the thermo-mechanical properties of a polymer material

An important aspect is to estimate the thermomechanical properties of a polymer system, in particular the glass transition temperature, Young's modulus and Poisson's ratio.

These properties are very important and their study is fundamental in many applications. These properties are determined by the atomic structure of the polymer and can therefore be derived by atomistic simulations.

Knowing these properties allows you to find limits such as the maximum operating temperature or the maximum applicable load. [18]

Glass Transition Temperature

The glass transition temperature is a very important property that characterizes polymer compounds. It is the temperature at which the polymer changes flexibility and more torsional movement of the polymer chain. In particular, the material changes from a solid glassy state to a more flexible rubbery one. As the temperature increases, the density decreases and when the glass transition temperature is exceeded, there is also a change in the rate of thermal expansion.

The glass transition temperature can be found from the change in the gradient of the density vs temperature graph. It is estimated using a simulated annealing process, where the material is cooled during an NPT molecular dynamics simulation.

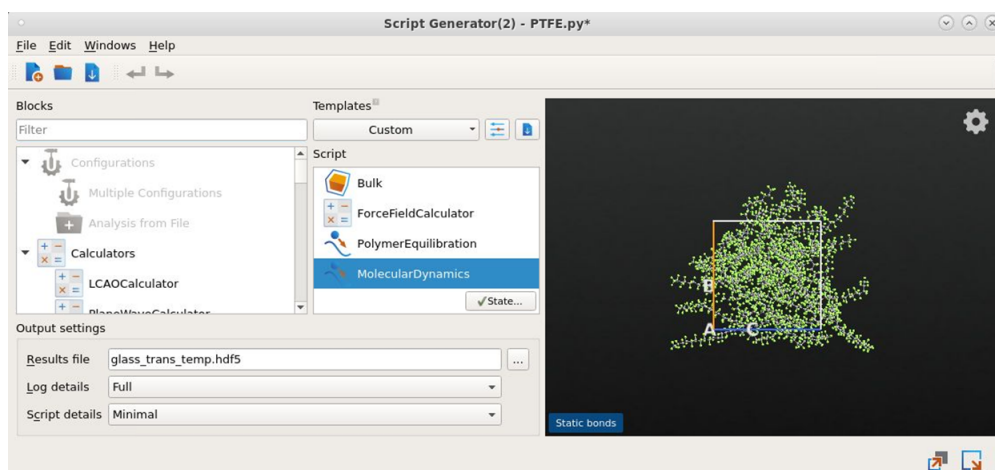


Figure 3.14. Script of the glass transition temperature simulation

In the Script is present the Bulk configuration, the Force Field Calculator, the PolymerEquilibration block and MolecularDynamics block.

OPLS-AA forcefield is added in the calculator block.

In PolymerEquilibration block, the most important parameter to set is the final temperature for equilibration. This temperature must be higher than the glass transition temperature in order to achieve the rate of thermal expansion above that temperature. This parameter has been set to 600K.

In the Molecular Dynamics block there are several changes to make.

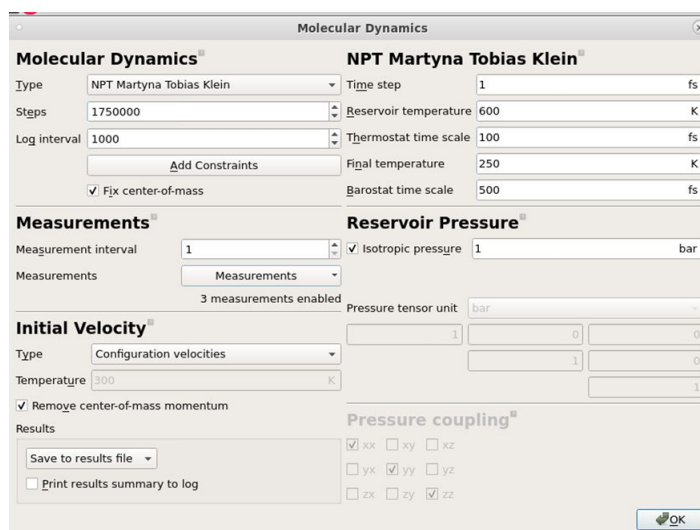


Figure 3.15. Molecular Dynamics parameters

- Select the NPT Martya Tobias Klein ensemble.
- Set the Steps to 1750000 and Log interval to 1000.
- In the Measurements section, add measurements for temperature, volume and density.
- Set the initial velocity to Configuration velocities.
- Set Reservoir temperature to 600K and Final temperature to 250K.

After the simulation, the glass transition temperature is obtained from the annealing trajectory.

The Glass Transition Temperature Analyzer tool is present with which it is possible to ascertain the trend of the density in relation to the temperature. The density trend can be approximated with two straight lines, one for low temperatures and one for high temperatures. The point of intersection of these two lines establishes the glass transition temperature. The tool automatically supplies the two lines with the validity limits and it is possible to manually modify the limits to obtain a better estimate of the glass transition temperature.

The glass transition temperature of PTFE

Polytetrafluoroethylene having 20 chains of 20 monomers was then analyzed.

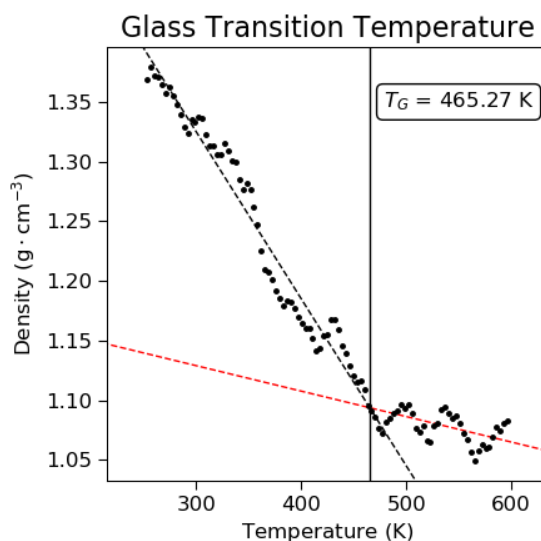


Figure 3.16. Glass Transition Temperature Analyzer of PTFE

As can be seen in the figure, the density decreases as the temperature increases. After the glass transition temperature, the density decreases much more slowly.

The glass transition temperature of PTFE is 465K, a low value typical of many polymers.

Young's Modulus and Poisson Ratio

Young's modulus is a measure of the amount of stress required to produce a given strain. It is simulated with the deformation which consists in progressively extending one of the lengths of the simulation cells using molecular dynamics. The resulting stress is recorded and the process is replicated in the three directions.

The gradient of the stress/strain curve gives the Young's modulus.

Young's modulus can change significantly with temperature, especially if the glass transition temperature is crossed. So it is useful to analyze the GTT simulation data and take a well-equilibrated structure at the initial temperature.

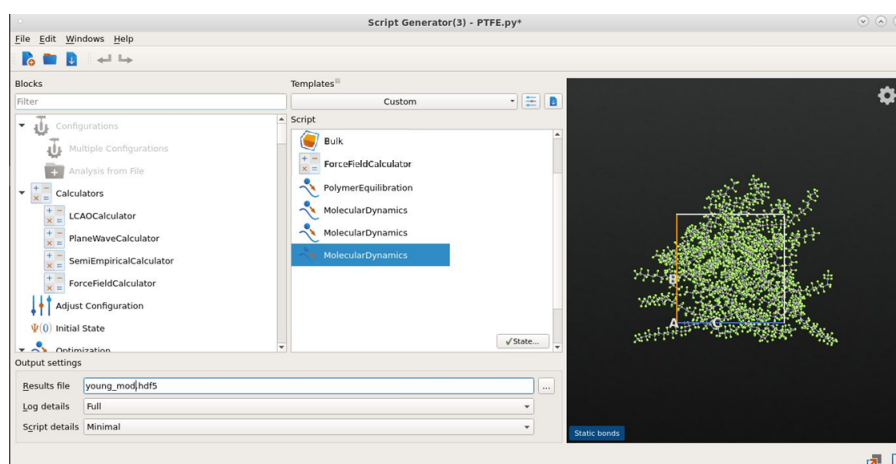


Figure 3.17. Young's modulus and Poisson ratio Script

In the script for the simulation of the Young's modulus and the Poisson Ratio there is the bulk configuration, the ForceFieldCalculator block, the PolymerEquilibration block and three MolecularDynamics blocks. For the ForceFieldCalculator the parameters are the same as the glass transition temperature. It is not necessary to change any PolymerEquilibration parameters since the system is equilibrated at room temperature. Different blocks of MolecularDynamics are used to simulate Young' modulus in different directions. In the Molecular Dynamics block, there are several changes to make.

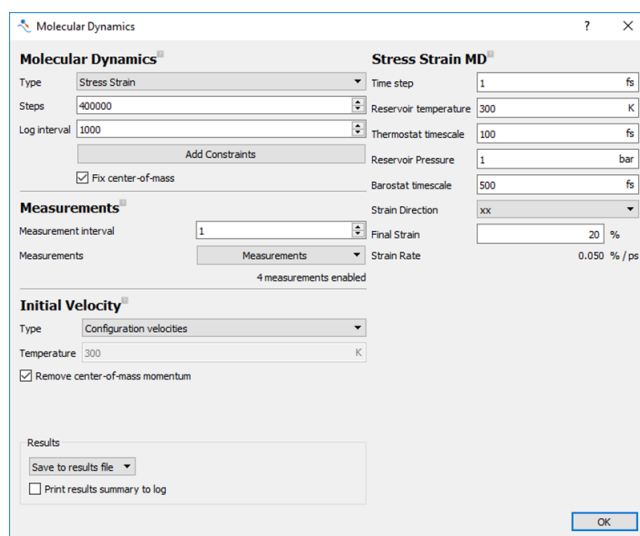


Figure 3.18. Young's modulus and Poisson ratio MolecularDynamics

- Set the Type to Stress Strain.
- Set Steps to 100000 and Log Interval to 1000.
- In the Measurements section, add all of the diagonal (xx, yy and zz) strains.
- In the Initial Velocity section, set Type to Configuration velocities.
- In the Stress Strain MD section, select the xx as the Strain Direction. Also set the the final strain to 20

The same parameters are set for the other two molecular dynamics blocks, only the strain direction is changed with yy and zz respectively.

The different simulations in the various directions are concatenated so the deformation in one direction is maintained and then the deformation in another direction is applied. The right thing is to analyze the behaviour in each direction starting from the initial configuration. To do this it is necessary to modify the script by removing the link from one simulation to the next.

After the simulation, the Young's modulus can be derived from the stress and strain data. You can use the Data Plot tool. On the x-axis the strain data is set in the xx direction while on the y-axis the stress data is also set in the xx direction.

In general, there is a large fluctuation in stress. This does not allow you to clearly derive the important information from the stress-strain graph.

To solve this problem an analysis can be done by rolling average of the data with a window of 1000. With the QuantumATK Graphic Editor, you can select the intervals in which the rolling average is done.

The resulting rolling average should in general be linear at low strain and then deviate

from linearity at high strain. To find the low strain gradient the polynomial fit analysis can be selected. By adapting the analysis interval and with the best approximation straight line it is, therefore, possible to calculate the Young's modulus.

The Poisson ratio is the ratio of the strain in the transverse direction to the applied strain. MDTrejectory saves the strain in each direction. Similarly to the Young's modulus, strain data can be plotted on a graph with best fit lines. The gradient of these lines is then the Poisson ratio.

Young's Modulus and Poisson Ratio of PTFE

The Young's modulus and Poisson's ratio were simulated for a configuration of polytetrafluoroethylene consisting of 20 chains of 20 monomers.

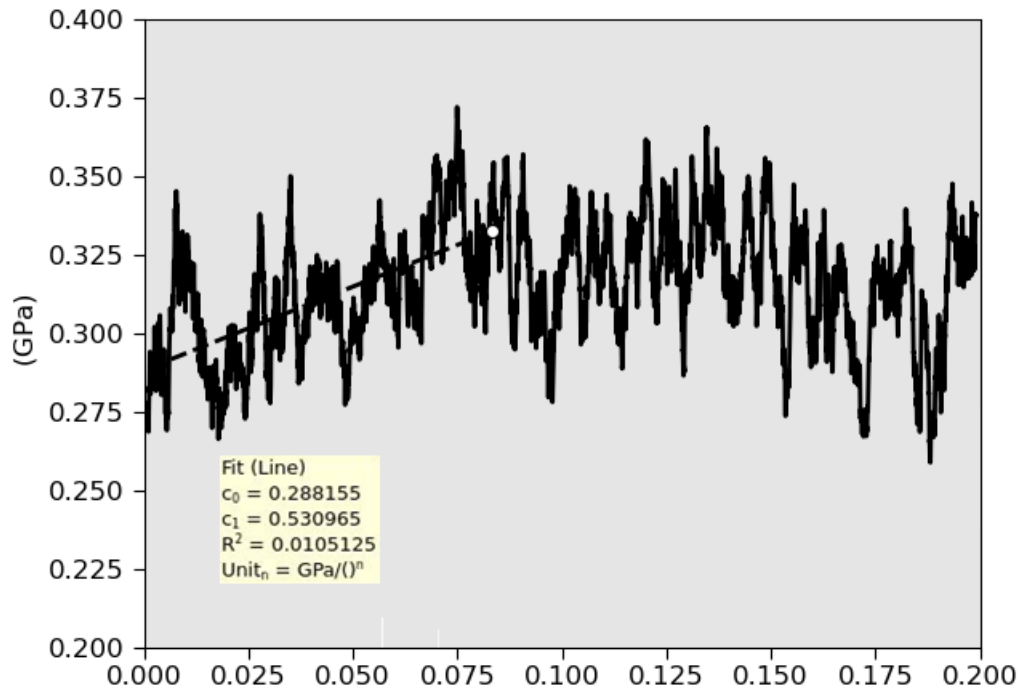


Figure 3.19. Young's modulus plot of PTFE

For PTFE the rolling average curve is fairly constant. In any case, there is a slight positive slope at low strain.

From the low strain polynomial fit, we can see the coefficient ' c_1 ' in the figure which corresponds to the gradient and therefore to the Young's modulus. However, the polynomial fit is very sensitive to the selected range.

The resulting Young's modulus is about 530 MPa.

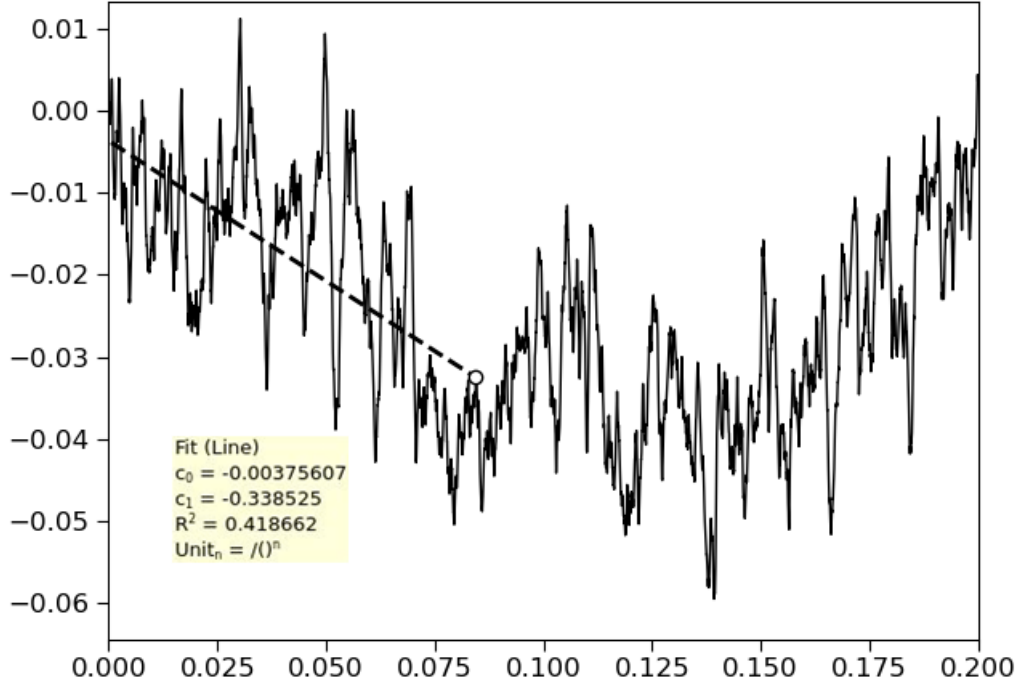


Figure 3.20. Poisson ratio plot of PTFE

Also in the Poisson ratio case the polynomial fit is very sensitive to the selected range. The Poisson's ratio is obtained from the absolute value of the coefficient 'c₁', about 0.34. Once the calculation is finished for each direction, there are three values of Young's modulus and 6 of Poisson ratio. It is possible to make an average to obtain the two parameters.

Specific heat capacity

The quantum harmonic oscillators model is used to calculate the specific heat capacity. The frequencies are determined using the vibrational density of states. [22] So the expression of the heat capacity is:

$$C_V(T) = \frac{h^2}{mk_B T^2} \int_0^\infty \frac{\nu^2 \exp(h\nu/k_B T)}{(\exp(h\nu/k_B T) - 1)^2} S(\nu) d\nu \quad (3.3)$$

where T is the temperature, ν is the vibrational frequency, h is Planck's constant, m is the total mass of the atoms in the unit cell, k_B is Boltzmann's constant, and $S(\nu)$ is the vibrational density of states.

Specific heat capacity of PTFE

The configuration PTFE_2_2, the ForceFieldCalculator and MolecularDynamics have been inserted in the QuantumATK script.

The following graph emerges from the simulation.

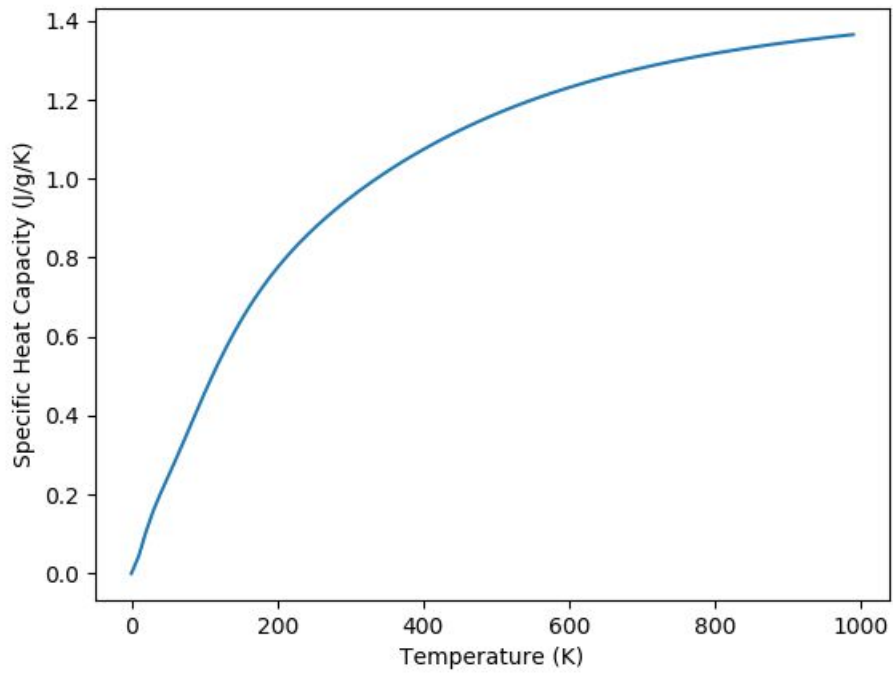


Figure 3.21. Specific heat capacity of PTFE

The specific heat capacity at 300K is $0.95 J \cdot g^{-1} \cdot K^{-1}$.

Chapter 4

Device simulations in Sentaurus TCAD

Sentaurus is a set of TCAD tools that simulate the fabrication processes, operation and reliability of semiconductor devices. Sentaurus simulators use physical models that allow optimization during wafer fabrication and in the analysis of the parameters that characterize the devices. Sentaurus tools combined enable a complete 2D and 3D simulation flow. [26]

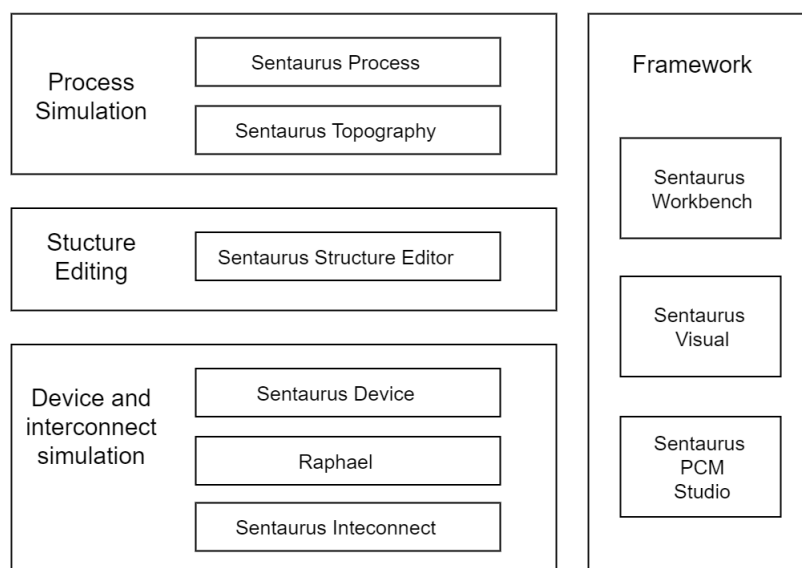


Figure 4.1. Sentaurus TCAD suite

Sentaurus Process allows you to simulate the various steps of the fabrication processes of 2D and 3D technologies. It uses advanced models for nanoscale simulations of CMOS

technology up to high-voltage power devices. Features an advanced set of oxidation, diffusion, implantation, and mechanics models, combined with robust mesh generation and structure-editing capabilities.

During the process, steps Sentaurus calculates all the main sources of mechanical stress due to volume changes, thermal and lattice misalignments and deposited thin films. The data of these stresses can be exported to make an analysis of the effects on electrical performance.

Sentaurus Topography simulates topography process steps such as deposition, etching, spin-on glass and reflow in 2-D and 3-D.

There are several models for the deposition process: Physical and Chemical vapor deposition (PVD and CVD), Plasma-enhanced chemical vapor deposition (PECVD), Low-pressure chemical vapor deposition (LPCVD) and others.

There are also different etching patterns including Wet etch, Reactive ion etch (RIE) and Chemical-mechanical polishing (CMP).

Sentaurus Structure Editor is a 2D and 3D device editor which builds and edits device structures using geometric operations.

Sentaurus Device simulates the electrical, thermal and optical characteristics of devices. It allows for the analysis of complex integrated circuit phenomena such as electrostatic discharge, latch-up, and single-event upset. Sentaurus Device through physical models and material parameters allows DC, AC, transient and harmonic equilibrium analysis. Models are included for physical effects such as stress- and orientation-dependent mobility, non-local tunneling, high-k dielectric mobility degradation, spatial quantization, and process-induced variability.

Raphael allows to simulate the electrical and thermal effects of the interconnections and allows the extraction of the resistance and capacitance parameters. Raphael also allows the automatic generation of interconnect structures.

Sentaurus Interconnect simulates the physical phenomena related to the device BEOL. Simulate different failures such as delamination, crack propagation, mechanical stress, Joule heating, electromigration and stress migration.

Sentaurus Workbench is the graphical environment for creating, managing, executing, and analyzing TCAD simulations.

Sentaurus Visual allows you to visualize the devices and data after the simulations. It allows a 3D view of the state of the art and visualizes the different sections.

Sentaurus PCM studio deals with the acquisition of multivariate process-device relationships using compact process models (PCM). PCMs capture the relationships between process variations and device performance through a variety of analytic functions.

4.1 NS-GAAFET simulation

The fabrication process steps of the NS-GAAFET device, described in chapter 2, were simulated with Sprocess.[25]

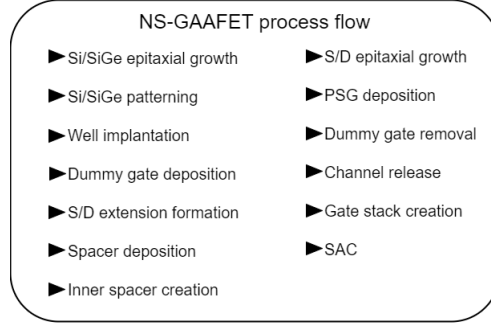


Figure 4.2. NS-GAAFET process flow

The device was simulated with the parameters described in the table, with different channel lengths and different source and drain doping concentrations.

Paramater	Value	Unit
Nanosheet height, H_{NS}	5	nm
Nanosheet channel gap	5	nm
Nanosheet width, W_{NS}	18	nm
STI thickness	22	nm
Spacer lenght, L_{SP}	8	nm
Gate lenght, L_g	12, 14, 18, 20	nm
S/D Doping, N_{SD}	$6 - 8 \times 10^{18}$	cm^{-3}
Channel dioing, N_{CH}	$9 \times 10^{16} - 1 \times 10^{17}$	cm^{-3}
Gate Stack		
Gate oxide (SiO_2)	0.7	nm
High- κ dielectric (HfO_2)	1	nm
Titanium nitride (TiN)	5	nm

Table 4.1. Sprocess NS-GAAFET parameters

The spacer is characterized by 8 nm thickness and simulations were done with different spacer materials.

The behaviour with silicon nitride ($\kappa = 7.5$), silicon dioxide ($\kappa = 3.9$) and finally PTFE ($\kappa = 2.5$) is analysed.

The electrical properties of the obtained devices were simulated with Sdevice.

In particular, I_{ON} and I_{OFF} are obtained from the I_D - V_{GS} curve in the saturation condition. I_{ON} is the current value I_D with $V_{DS} = V_{DD}$ and $V_{GS} = V_{DD}$ and I_{OFF} is the

current value I_D with $V_{DS} = V_{DD}$ and $V_{GS} = 0V$.

Important figures of merit of the transistor are the threshold voltage V_{TH} , The subthreshold slope SS and the drain-induced barrier lowering $DIBL$.

The threshold voltage is obtained from the I_D - V_{GS} curve in linear condition using the maximum transconductance method. With this method, V_{TH} is defined as the intersection of the tangent at the maximum transconductance point ($g_m = dI_D/dV_{GS}$) with the gate voltage.

The SS indicates how easily a transistor is turned off. Indicates the variation of the gate voltage to decrease/increase the sub-threshold current by one order of magnitude.

$$SS = \ln(10) \frac{kT}{q} \left(1 + \frac{C_d}{C_{ox}} \right) \quad (4.1)$$

with C_d the depletion layer and C_{ox} gate-oxide capacitance.

A good transistor has a low subthreshold swing value and the minimum value of a conventional device can be found by letting $C_d \rightarrow 0$ and $C_{ox} \rightarrow \infty$.

$$SS = \ln(10) \frac{kT}{q} \quad (4.2)$$

It is known as the thermionic limit and is 60 mV/dec at room temperature (300 K).

With Sdevice the SS parameter is extracted from the I_D - V_{GS} curve through the following equation

$$SS = \left(\frac{d \log_{10}(I_D)}{dV_{GS}} \right)^{-1} \quad (4.3)$$

The SS value must be calculated at V_{GS} lower than V_{TH} but not close to 0V, therefore a value in the middle.

The analyzed device has a channel length of a few nanometers, therefore it is subject to short channel effects. Consequently, the threshold voltage decreases as the drain voltage increases.

As drain voltage is increased, the depletion region of the p-n junction between the drain and body increases in size and extends under the gate.

In order to balance the charge, the gate is forced to attract more carriers towards itself from the channel, an effect that results in the lowering of the threshold voltage.

In other words, the potential energy barrier for electrons in the channel is lowered. Hence the term "drain-induced barrier lowering" is used to describe the phenomenon.

The $DIBL$ value is derived from the following equation:

$$DIBL = - \frac{V_{th}^{DD} - V_{th}^{low}}{V_{DD} - V_D^{low}} \quad (4.4)$$

where V_{th}^{DD} is the threshold voltage with the drain voltage equal to the supply voltage V_{DD} and V_{th}^{low} is the threshold voltage with the drain voltage equal to a low value V_D^{low} .

A key aspect of device performance is the I_{ON}/I_{OFF} ratio which must be high enough.

4.1.1 n-type NS-GAAFET

In the figure, the device obtained from the Sprocess simulation. The device was developed from Luca Scognamiglio's thesis work with the addition of some modifications.[25]

A generic SpacerMaterial has been defined to then insert the parameters of nitride, oxide or PTFE in the Sdevice simulations.

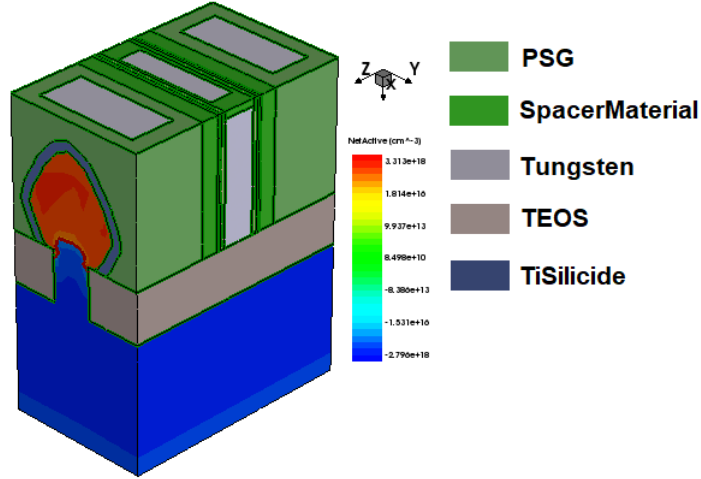


Figure 4.3. n-type GAAFET device at the end of the Sprocess simulation

The Sdevice simulations were carried out with this device. The DC characteristics of the device were first analyzed. It was found that the spacer material has little effect on the DC characteristics.

The characteristics of the device with nitride as spacer material are reported.

In figure 4.4, the characteristic of the I_D - V_{GS} curve for the different channel lengths with $V_{DS} = 0.05V$, therefore in the linear region. The curves are very similar, as L_g decreases, a slight upward shift can be seen.

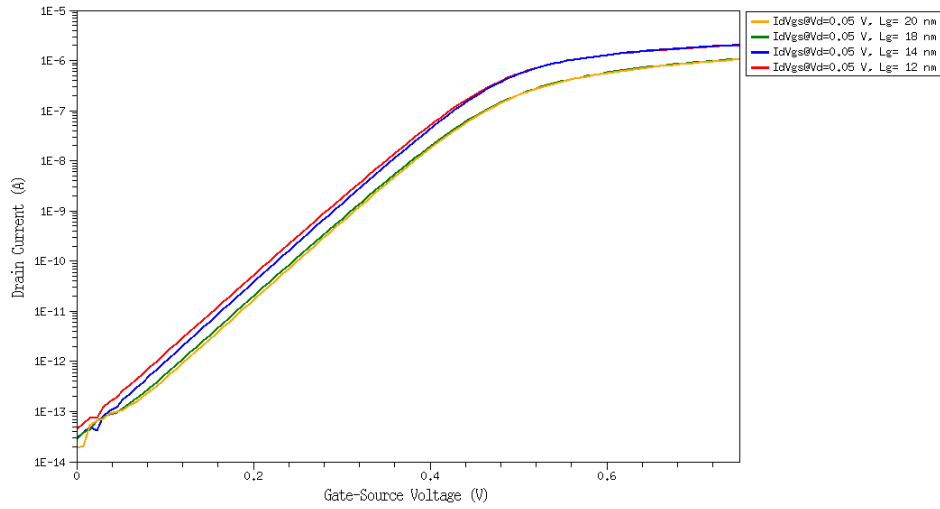


Figure 4.4. I_D - V_{GS} curves of n-type NS-GAAFET in linear regime.

In figure 4.5, the characteristic of the I_D - V_{GS} curve for the different channel lengths with $V_{DS} = 0.75V$, therefore in the saturation region. In this case the curves are less similar than the linear condition.

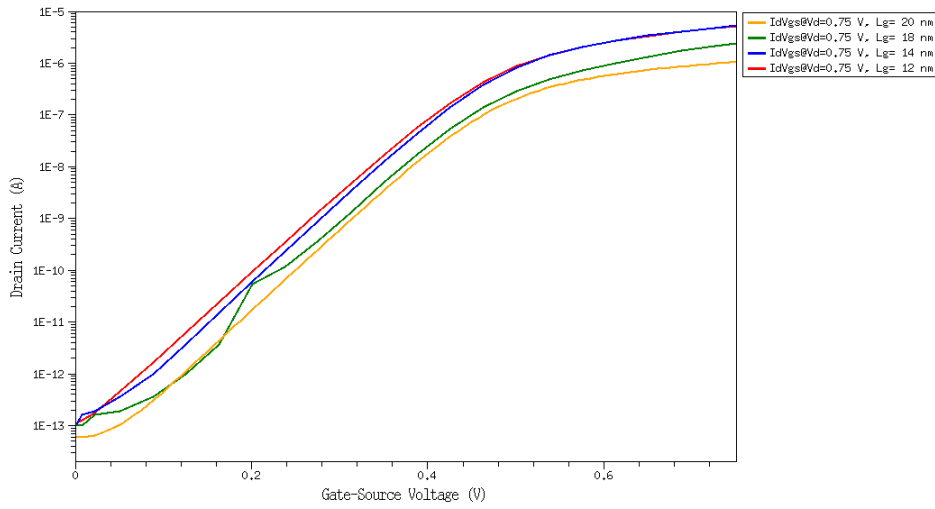
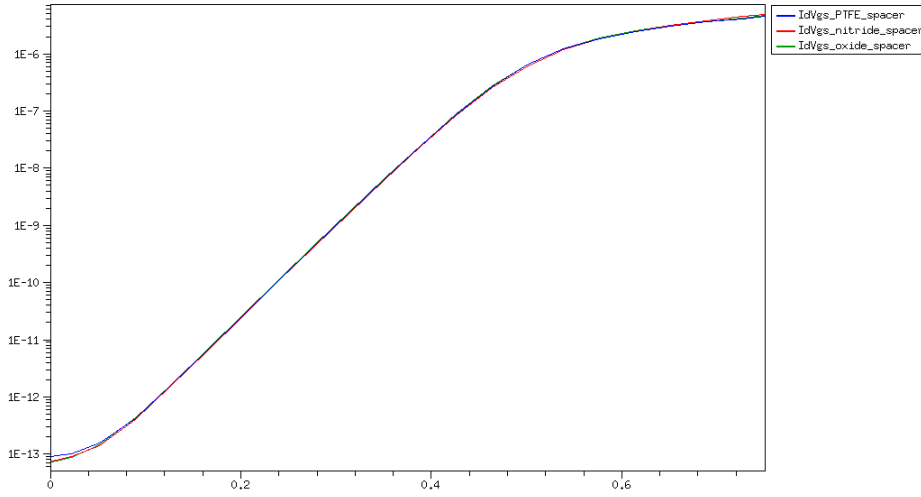


Figure 4.5. I_D - V_{GS} curves of n-type NS-GAAFET in saturation regime.

The data shown in the table 4.2 are extrapolated from the I_D - V_{GS} curves obtained in linear and saturation regimes.

n-type NS-GAAFET $V_{DD}=0.75$ V				
Parameters	Values			
Lg (nm)	12	14	18	20
V_{TH} (V)	0.43	0.44	0.45	0.45
I_{ON} (μ A)	5.19	5.11	4.15	3.05
I_{OFF} (pA)	0.11	0.10	0.08	0.06
I_{ON}/I_{OFF}	4.86×10^7	5.06×10^7	5.20×10^7	5.26×10^7
SS (mV/dec)	74.60	74.45	73.90	73.38
DIBL (mV/V)	41.02	35.16	34.30	30.27

Table 4.2. Parameters of n-type NSGAAFET with different channel lengths

Figure 4.6. I_D - V_{GS} curves of n-type NS-GAAFET in saturation for different spacer materials

In figure 4.6, the I_D - V_{GS} curves are reported for the device with $L_g=20$ nm for the different configurations of spacer material (nitride, oxide and PTFE). The curves are very similar so the spacer material does not affect the static characteristics of the device.

4.1.2 p-type NS-GAAFET

In the figure, the device obtained from the Sprocess simulation.

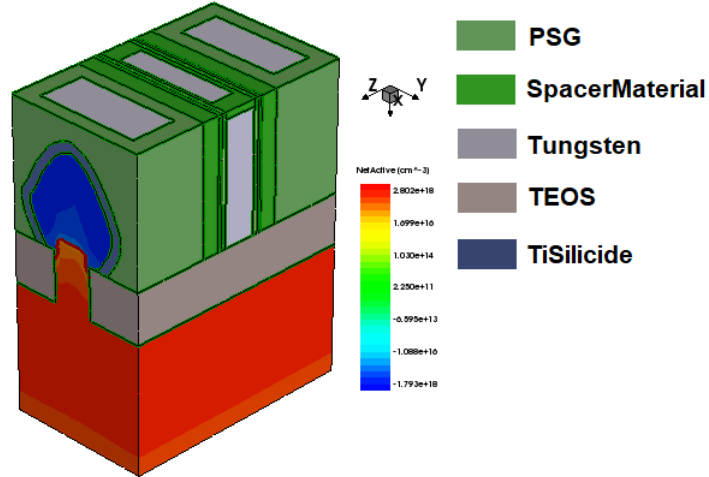


Figure 4.7. p-type GAAFET device at the end of the Sprocess simulation

Similarly n-type, also for the p-type, it was found that the spacer material has little effect on the DC characteristics.

The characteristics of the device with nitride as spacer material are reported.

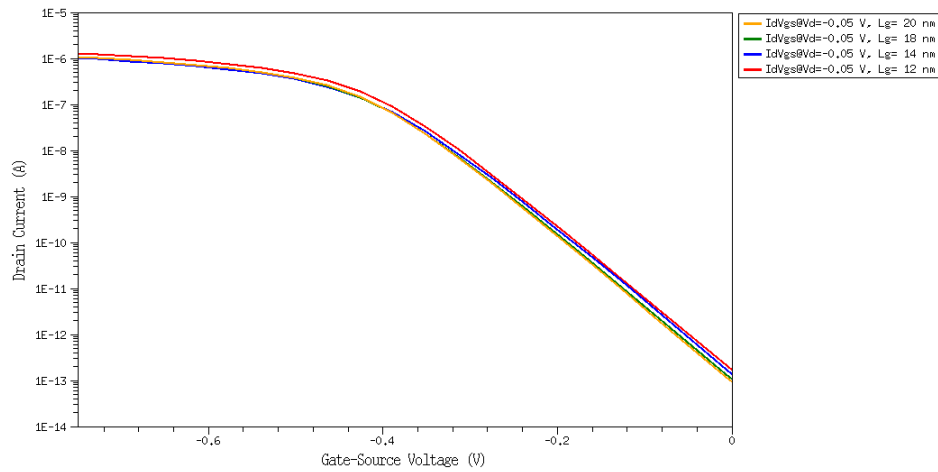


Figure 4.8. I_D - V_{GS} curves of p-type NS-GAAFET in linear regime.

In figure 4.8, the characteristic of the I_D - V_{GS} curve for the different channel lengths with $V_{DS} = -0.05V$, therefore in the linear region.

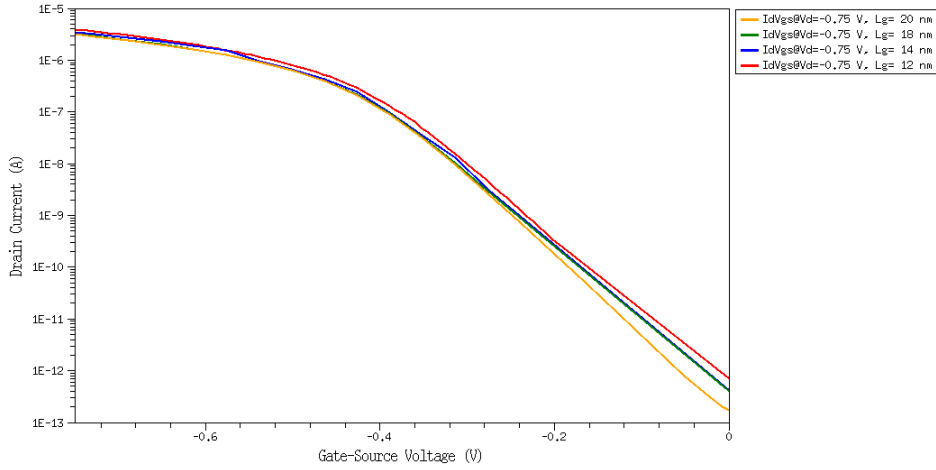


Figure 4.9. I_D - V_{GS} curves of p-type NS-GAAFET in saturation regime.

In figure 4.9, the characteristic of the I_D - V_{GS} curve for the different channel lengths with $V_{DS} = -0.75\text{V}$, therefore in the saturation region. Fewer differences than n-type NSGAAFET can be observed in both the linear region and the saturation region.

p-type NS-GAAFET $V_{DD}=-0.75\text{ V}$				
Parameters	Values			
L_g (nm)	12	14	18	20
V_{TH} (V)	-0.38	-0.38	-0.38	-0.39
I_{ON} (μA)	-3.90	-3.39	-3.19	-3.18
I_{OFF} (pA)	-0.69	-0.42	-0.39	-0.17
I_{ON}/I_{OFF}	5.68×10^6	8.01×10^6	8.12×10^6	1.88×10^7
SS (mV/dec)	77.09	76.18	75.59	69.04
DIBL (mV/V)	47.16	46.97	39.26	35.40

Table 4.3. Parameters of p-type NSGAAFET with different channel lengths

The table 4.3 shows the parameters obtained from the I_D - V_{GS} curves for the p-type NS-GAAFET device.

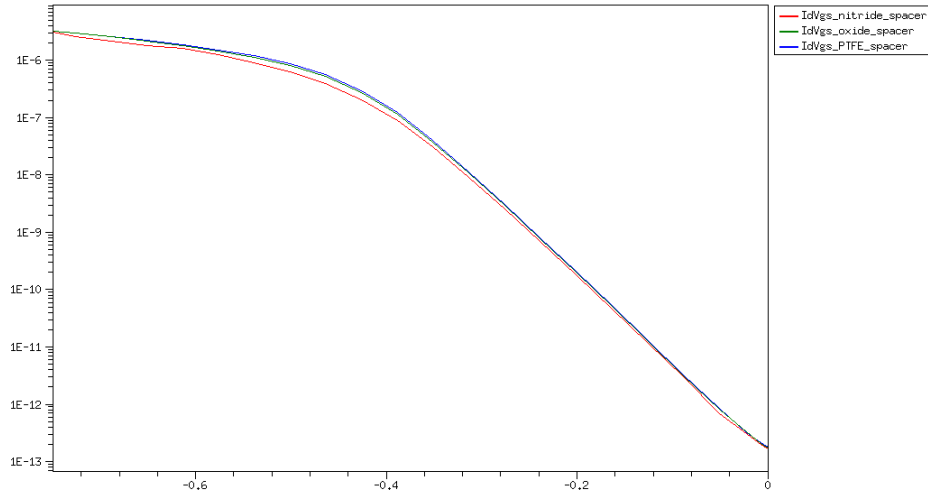


Figure 4.10. I_D - V_{GS} curves of p-type NS-GAAFET in saturation for different spacer materials

In figure 4.10, the I_D - V_{GS} curves are reported for the device with $L_g=20\text{nm}$ for the different configurations of spacer material (nitride, oxide and PTFE). As expected, also in this case, the curves are very similar so the spacer material does not affect the static characteristics of the device.

4.2 NS-GAAFET frequency response

When the value of κ of the spacer decreases, the NS-GAAFET device does not significantly change the DC characteristics. An AC performance analysis can be performed to investigate possible benefits of having low- κ dielectric as a spacer material.

The NS-GAAFET can be considered a 4-port device: gate, source, drain and substrate. Among these 4 ports, only the gate and the drain are of particular interest. Indeed, the source is at the reference voltage and can be used as a common terminal and the substrate is isolated from the rest of the device. [14]

So it can be considered:

- port 1 the gate and the source of the device
- port 2 the drain and the source of the device

To proceed to a frequency analysis it is necessary to analyze the small signal equivalent circuit. [28]

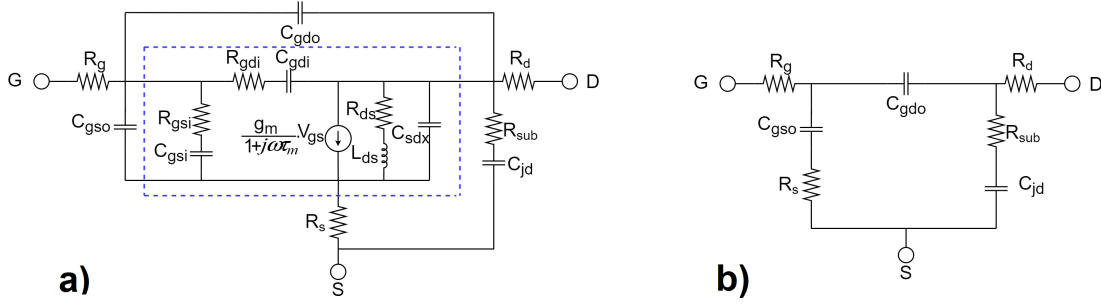


Figure 4.11. Small signal equivalent circuit NS-GAAFET a) ON-state , b) OFF-state

In the figure the small signal equivalent circuits. In the figure a) the ON-state circuit where what is included in the blue dashed line is bias-dependent, while in the figure b) the OFF-state circuit.

The elements of the circuits represent:

- C_{gdo} and C_{gso} are the capacitance between the gate and source/drain.
- R_g , R_s , R_d and R_{sub} are the resistance of the gate, source, drain and substrate.
- C_{jd} is the capacitance between the drain and substrate.
- C_{gsi} and C_{gdi} are the capacitance between the source/drain overlap and gate region.
- R_{gsi} and R_{gdi} are the resistance of the source and drain overlap region.
- R_{ds} and L_{ds} are the channel's resistance and inductance.
- τ_m is the transmission delay between source and drain.
- C_{sdx} represents the DIBL effect.
- g_m is the transconductance.

An interesting parameter of AC performance is the current cutoff frequency. It is the frequency, f_T , at which the current transfer function $H_{21}(f_T)$ between the gate current and the drain current is 1.

$$H_{21}(f) = \left. \frac{i_{ds}}{i_{gs}} \right|_{v_{ds}=0} = \frac{Y_{21}(f)}{Y_{11}(f)} \quad (4.5)$$

With Sentaurus device it is possible to obtain the current cutoff frequency and extract the various parameters that characterize the small signal circuit.

This part of the simulation has not been completed. Therefore this represents the introduction of a work that could prove the benefits of low- κ materials as spacer materials.

Chapter 5

Conclusions and future research

This work is aimed at introducing new low- κ dielectric materials into transistor fabrication processes.

In this study the attention is placed on the NS-GAAFET device and in particular on the dielectric structure of the spacer and inner spacer in the FEOL.

The starting point was the analysis of low- κ materials, of the methods of reduction of the dielectric constant with the introduction of pores and of the mechanical and thermal properties which are the weak point of these materials. It emerged that polymers represent the materials with the lowest κ value.

Among the polymers of particular interest is polytetrafluoroethylene, PTFE, due to the low dielectric constant value of about 2.5.

QuantumATK has made it possible to atomistically analyze this material by obtaining the dielectric constant, the glass transition temperature, Young's modulus, Poisson ratio and the specific heat capacity.

As with most polymers, QATK simulations of PTFE confirmed the low- κ value and worse mechanical and thermal properties compared to silicon nitride and silicon dioxide which are the main materials used as dielectrics in transistors.

Once the properties of the PTFE were obtained, we proceeded with the fabrication and simulations of the static performance of the NS-GAAFET device using the Sentaurus process and Sentaurus device.

The NS-GAAFET n-type and p-type devices were made with different spacer materials: silicon nitride, silicon dioxide and PTFE. From the static simulations of the device the main parameters such as I_{ON} , I_{OFF} , V_{TH} , SS and DIBL were obtained but no substantial differences emerged between the devices with the different spacer materials.

It is necessary to carry out some AC simulations to quantify the benefits that a low- κ value material used as a spacer material can bring. The latter simulations have not been completed in this work.

This work can be further developed and improved into a more in-depth analysis of the

polymer material using QuantumATK. There are important properties that can be simulated such as electrical resistivity, band structure and thermal conductivity.

From the point of view of the NS-GAAFET device, in addition to the completion of the AC simulations, mechanical and thermal simulations can be made which are expected to present a worse behavior than the classical dielectrics.

This method of proceeding, first with atomistic simulations of the newly introduced material and then with device analysis, can be used to investigate promising new dielectric materials that have been presented in this work.

Besides the spacer and inner spacer structure low- κ dielectric materials can be used and investigated also in other structures such as STI in FEOL or ILD in BEOL.

Appendix A

Insight into QuantumATK classes

This section contains the Python scripts of the different simulations executed. Bulk configuration section is omitted describing atom coordinates, bonds and tags.

A.1 Dielectric tensor analysis Python script

```
1 # -*- coding: utf-8 -*-
2 # -----
3 # Bulk Configuration
4 # -----
5 ...
6 ...
7 ...
8 # -----
9 # Calculator
10 # -----
11 #-----
12 # Basis Set
13 #-----
14 basis_set = [
15     GGABasis.Carbon_DoubleZetaPolarized,
16     GGABasis.Fluorine_DoubleZetaPolarized,
17 ]
18
19 k_point_sampling = KpointDensity(
20     density_a=4.0*Angstrom,
21 )
22 numerical_accuracy_parameters = NumericalAccuracyParameters(
23     density_mesh_cutoff=80.0*Hartree,
24     k_point_sampling=k_point_sampling,
```

```
25     )
26
27 poisson_solver = ParallelConjugateGradientSolver(
28     boundary_conditions=[[PeriodicBoundaryCondition(),
29                          PeriodicBoundaryCondition()],
30                          [PeriodicBoundaryCondition(),
31                          PeriodicBoundaryCondition()],
32                          [PeriodicBoundaryCondition(),
33                          PeriodicBoundaryCondition()]]
34 )
35
36 #-----
37 # Grimme DFTD3
38 #-----
39 correction_extension = GrimmeDFTD3(
40     exchange_correlation=GGA.PBE,
41     maximum_neighbour_distance=30.0*Ang,
42     include_three_body_term=False,
43 )
44
45 calculator = LCAOcalculator(
46     basis_set=basis_set,
47     numerical_accuracy_parameters=numerical_accuracy_parameters,
48     poisson_solver=poisson_solver,
49     correction_extension=correction_extension,
50 )
51
52 bulk_configuration.setCalculator(calculator)
53 nlprint(bulk_configuration)
54 bulk_configuration.update()
55 nlsave('PTFE_2_2_dt_sim_2_1.hdf5', bulk_configuration)
56
57 # -----
58 # Optimize Geometry
59 # -----
60 bulk_configuration = OptimizeGeometry(
61     bulk_configuration,
62     max_forces=0.001*eV/Ang,
63     max_steps=500,
64     max_step_length=0.2*Ang,
65     trajectory_filename='PTFE_2_2_dt_sim_2_1_trajectory.hdf5',
66     trajectory_interval=5.0*Minute,
67     restart_strategy=RestartFromTrajectory(),
68     disable_stress=True,
69     optimizer_method=LBFGRS(),
70     enable_optimization_stop_file=True,
71 )
72 nlsave('PTFE_2_2_dt_sim_2_1.hdf5', bulk_configuration)
```

```
73 nlprint(bulk_configuration)
74
75 # -----
76 # Dynamical Matrix
77 # -----
78 dynamical_matrix = DynamicalMatrix(
79     bulk_configuration,
80     filename='PTFE_2_2_dt_sim_2_1.hdf5',
81     object_id='dynamical_matrix',
82     repetitions=(1, 1, 1),
83     atomic_displacement=0.01*Angstrom,
84     acoustic_sum_rule=True,
85     finite_difference_method=Central,
86     force_tolerance=1e-08*Hartree/Bohr**2,
87     processes_per_displacement=None,
88     log_filename_prefix='forces_displacement_',
89     use_wigner_seitz_scheme=True,
90 )
91 dynamical_matrix.update()
92
93 # -----
94 # Optical Spectrum
95 # -----
96 kpoint_grid = KpointDensity(
97     density_a=7.0*Angstrom,
98 )
99
100 optical_spectrum = OpticalSpectrum(
101     configuration=bulk_configuration,
102     kpoints=kpoint_grid,
103     energies=numpy.linspace(0, 0.17, 501)*eV,
104     broadening=0.1*eV,
105     bands_below_fermi_level=200,
106     bands_above_fermi_level=200,
107     method=Full,
108 )
109 nlsave('PTFE_2_2_dt_sim_2_1.hdf5', optical_spectrum)
110
111 # -----
112 # Born Effective Charge
113 # -----
114 born_effective_charge = BornEffectiveCharge(
115     configuration=bulk_configuration,
116     kpoints_a=MonkhorstPackGrid(11, 5, 5),
117     kpoints_b=MonkhorstPackGrid(5, 11, 5),
118     kpoints_c=MonkhorstPackGrid(5, 5, 11),
119     atomic_displacement=0.01*Angstrom,
120 )
```

```

121 nlsave('PTFE_2_2_dt_sim_2_1.hdf5', born_effective_charge)
122
123 # -----
124 # Dielectric Tensor
125 # -----
126 dielectric_tensor = DielectricTensor(
127     configuration=bulk_configuration,
128     dynamical_matrix=dynamical_matrix,
129     optical_spectrum=optical_spectrum,
130     born_effective_charge=born_effective_charge,
131 )
132 nlsave('PTFE_2_2_dt_sim_2_1.hdf5', dielectric_tensor)

```

A.2 Glass transition temperature Python script

```

1 # -*- coding: utf-8 -*-
2 # -----
3 # Bulk Configuration
4 # -----
5 ...
6 ...
7 ...
8 # -----
9 # Calculator
10 # -----
11 potential_builder = OPLSPotentialBuilder(
12     use_bonds=True,
13     include_bond_stretching=True,
14     include_bond_angles=True,
15     include_torsions=True,
16     include_inversions=True,
17     include_lennard_jones=True,
18     include_electrostatic=True,
19     lennard_jones_cutoff=10.0*Angstrom,
20     lennard_jones_smoothing_length=2.0*Angstrom,
21     electrostatic_pairwise_cutoff=12.0*Angstrom,
22     electrostatic_smoothing_length=2.0*Angstrom,
23     electrostatic_spme_cutoff=7.5*Angstrom,
24     electrostatic_accuracy=0.0001,
25     electrostatic_scale=1.0,
26     use_electrostatic_direct_sum=False,
27     ignore_missing_types=False,
28 )
29 calculator = potential_builder.createCalculator(bulk_configuration)
30
31 bulk_configuration.setCalculator(calculator)

```

```
32 nlprint(bulk_configuration)
33 bulk_configuration.update()
34 nlsave('PTFE_GTT.hdf5', bulk_configuration)
35
36 # -----
37 # Polymer Equilibration
38 # -----
39 polymer_equilibration = PolymerEquilibration(
40     bulk_configuration,
41     filename='PTFE_GTT.hdf5',
42     object_id='polymer_equilibration',
43     log_filename_prefix='polymer_equilibration_',
44     max_temperature=1000.0*Kelvin,
45     final_temperature=600.0*Kelvin,
46     max_pressure=5.0*GPa,
47     final_pressure=1.0*bar,
48     isotropic_pressure=True,
49     time_scale_factor=1.000,
50     log_interval=100,
51     trajectory_interval=1000,
52 )
53 polymer_equilibration.update()
54
55 bulk_configuration = polymer_equilibration.equilibratedConfiguration()
56 nlsave('PTFE_GTT.hdf5', bulk_configuration)
57
58
59 # -----
60 # Molecular Dynamics
61 # -----
62
63 initial_velocity = ConfigurationVelocities(
64     remove_center_of_mass_momentum=True,
65 )
66
67 method = NPTMartynaTobiasKlein(
68     time_step=1*femtoSecond,
69     reservoir_temperature=600*Kelvin,
70     reservoir_pressure=1*bar,
71     thermostat_timescale=100*femtoSecond,
72     barostat_timescale=500*femtoSecond,
73     initial_velocity=initial_velocity,
74     heating_rate=-0.2*Kelvin/picoSecond,
75     compression_rate=0*bar/femtoSecond,
76     chain_length=3,
77 )
78
79 constraints = [FixCenterOfMass()]
```

```
80
81 measurement_names = ['temperature', 'volume', 'density']
82
83 md_trajectory = MolecularDynamics(
84     bulk_configuration,
85     constraints=constraints,
86     trajectory_filename='PTFE_GTT.hdf5',
87     steps=1750000,
88     log_interval=1000,
89     measurement_hook=MDMeasurement(measurement_names, call_interval=1),
90     method=method
91 )
92
93 bulk_configuration = md_trajectory.lastImage()
```

A.3 Young's modulus and Poisson ratio Python script

```
1 # -*- coding: utf-8 -*-
2 # -----
3 # Bulk Configuration
4 # -----
5 ...
6 ...
7 ...
8 # -----
9 # Calculator
10 # -----
11 potential_builder = OPLSPotentialBuilder(
12     use_bonds=True,
13     include_bond_stretching=True,
14     include_bond_angles=True,
15     include_torsions=True,
16     include_inversions=True,
17     include_lennard_jones=True,
18     include_electrostatic=True,
19     lennard_jones_cutoff=10.0*Angstrom,
20     lennard_jones_smoothing_length=2.0*Angstrom,
21     electrostatic_pairwise_cutoff=12.0*Angstrom,
22     electrostatic_smoothing_length=2.0*Angstrom,
23     electrostatic_spme_cutoff=7.5*Angstrom,
24     electrostatic_accuracy=0.0001,
25     electrostatic_scale=1.0,
26     use_electrostatic_direct_sum=False,
27     ignore_missing_types=False,
28 )
29 calculator = potential_builder.createCalculator(bulk_configuration)
```

```
30
31 bulk_configuration.setCalculator(calculator)
32 nlprint(bulk_configuration)
33 bulk_configuration.update()
34 nlsave('PTFE_young.hdf5', bulk_configuration)
35
36 # -----
37 # Polymer Equilibration
38 # -----
39 polymer_equilibration = PolymerEquilibration(
40     bulk_configuration,
41     filename='PTFE_young.hdf5',
42     object_id='polymer_equilibration',
43     log_filename_prefix='polymer_equilibration_',
44     max_temperature=1000.0*Kelvin,
45     final_temperature=300.0*Kelvin,
46     max_pressure=5.0*GPa,
47     final_pressure=1.0*bar,
48     isotropic_pressure=True,
49     time_scale_factor=1.000,
50     log_interval=100,
51     trajectory_interval=1000,
52 )
53 polymer_equilibration.update()
54
55 bulk_configuration = polymer_equilibration.equilibratedConfiguration()
56 nlsave('PTFE_young.hdf5', bulk_configuration)
57
58
59 # -----
60 # Molecular Dynamics
61 # -----
62
63 initial_velocity = ConfigurationVelocities(
64     remove_center_of_mass_momentum=True,
65 )
66
67 method = NPTMartynaTobiasKlein(
68     time_step=1*femtoSecond,
69     reservoir_temperature=300*Kelvin,
70     reservoir_pressure=[0, 1, 1, 0, 0, 0]*bar,
71     thermostat_timescale=100*femtoSecond,
72     barostat_timescale=500*femtoSecond,
73     initial_velocity=initial_velocity,
74     heating_rate=0*Kelvin/picoSecond,
75     compression_rate=0*bar/femtoSecond,
76     coupling_mask=[[False, False, False], [False, True, False], [False,
↵ False, True]],
```

```

77     chain_length=3,
78 )
79
80 strain_configuration_hook = StrainConfigurationHook(
81     strain_direction='xx',
82     strain_rate=0.002/picoSecond,
83 )
84
85 constraints = [FixCenterOfMass()]
86
87 measurement_names = ['stress_xx', 'strain_xx', 'strain_yy', 'strain_zz']
88
89 md_trajectory = MolecularDynamics(
90     bulk_configuration,
91     constraints=constraints,
92     trajectory_filename='PTFE_young.hdf5',
93     steps=100000,
94     log_interval=1000,
95     pre_step_hook=strain_configuration_hook,
96     measurement_hook=MDMeasurement(measurement_names, call_interval=1),
97     method=method
98 )
99
100 # -----
101 # Molecular Dynamics
102 # -----
103
104 initial_velocity = ConfigurationVelocities(
105     remove_center_of_mass_momentum=True,
106 )
107
108 method = NPTMartynaTobiasKlein(
109     time_step=1*femtoSecond,
110     reservoir_temperature=300*Kelvin,
111     reservoir_pressure=[1, 0, 1, 0, 0, 0]*bar,
112     thermostat_timescale=100*femtoSecond,
113     barostat_timescale=500*femtoSecond,
114     initial_velocity=initial_velocity,
115     heating_rate=0*Kelvin/picoSecond,
116     compression_rate=0*bar/femtoSecond,
117     coupling_mask=[[True, False, False], [False, False, False], [False,
118     ↪ False, True]],
119     chain_length=3,
120 )
121
122 strain_configuration_hook = StrainConfigurationHook(
123     strain_direction='yy',
124     strain_rate=0.002/picoSecond,

```

```

124 )
125
126 constraints = [FixCenterOfMass()]
127
128 measurement_names = ['stress_yy', 'strain_yy', 'strain_zz']
129
130 md_trajectory = MolecularDynamics(
131     bulk_configuration,
132     constraints=constraints,
133     trajectory_filename='PTFE_young.hdf5',
134     steps=100000,
135     log_interval=1000,
136     pre_step_hook=strain_configuration_hook,
137     measurement_hook=MDMeasurement(measurement_names, call_interval=1),
138     method=method
139 )
140
141 # -----
142 # Molecular Dynamics
143 # -----
144
145 initial_velocity = ConfigurationVelocities(
146     remove_center_of_mass_momentum=True,
147 )
148
149 method = NPTMartynaTobiasKlein(
150     time_step=1*femtoSecond,
151     reservoir_temperature=300*Kelvin,
152     reservoir_pressure=[1, 1, 0, 0, 0, 0]*bar,
153     thermostat_timescale=100*femtoSecond,
154     barostat_timescale=500*femtoSecond,
155     initial_velocity=initial_velocity,
156     heating_rate=0*Kelvin/picoSecond,
157     compression_rate=0*bar/femtoSecond,
158     coupling_mask=[[True, False, False], [False, True, False], [False,
↵ False, False]],
159     chain_length=3,
160 )
161
162 strain_configuration_hook = StrainConfigurationHook(
163     strain_direction='zz',
164     strain_rate=0.002/picoSecond,
165 )
166
167 constraints = [FixCenterOfMass()]
168
169 measurement_names = ['stress_zz', 'strain_yy', 'strain_zz']
170

```

```
171 md_trajectory = MolecularDynamics(  
172     bulk_configuration,  
173     constraints=constraints,  
174     trajectory_filename='PTFE_young.hdf5',  
175     steps=100000,  
176     log_interval=1000,  
177     pre_step_hook=strain_configuration_hook,  
178     measurement_hook=MDMeasurement(measurement_names, call_interval=1),  
179     method=method  
180 )  
181  
182 bulk_configuration = md_trajectory.lastImage()
```

Appendix B

Definition of thermal and mechanical parameters

B.1 Glass Transition Temperature

The glass transition temperature, T_g , is the temperature at which an amorphous polymer moves from a hard or glassy state to a softer, rubbery or viscous state. [6]

The glass transition temperature is an important thermal property for plastics and polymers because these materials do not behave like traditional solids and liquids.

B.2 Young's modulus

Young's modulus is a mechanical property of materials that quantifies how easily a material can stretch and deform. It is defined as the ratio of tensile stress to tensile strain. [15]

B.3 Poisson's ratio

When a material is stretched or compressed the Poisson ratio measure the ratio of a material's transverse strain to its longitudinal strain.

Poisson's ratio is taken with a positive sign and is in the range 0-0.5. [4]

Bibliography

- [1] International roadmap for devices and system 2022 edition executive summary. *IEEE*, 2022.
- [2] M. Amato. Nanosheet-gaafets modeling and circuit performance evaluation. *Master Thesis*, 2021.
- [3] Yi-Lung Cheng and Chih-Yen Lee. Porous low-dielectric-constant material for semiconductor microelectronics. In Mohsen Sheikholeslami Kandelousi, Sadia Ameen, M. Shaheer Akhtar, and Hyung-Shik Shin, editors, *Nanofluid Flow in Porous Media*, chapter 11. IntechOpen, Rijeka, 2018.
- [4] Kamal Dwivedi. Poisson’s ratio: Definition, formula, unit, calculation. <https://www.mechical.com/2022/09/poissons-ratio.html>.
- [5] D. De Rossi F. Carpi. *Fenomeni Bioelettrici, capitolo 5, Campi elettrici nella materia: polarizzazione di dielettrici ideali e con perdite*. centropiaggio.unipi.
- [6] Dan Griffin. What is the glass transition temperature (tg) of a polymer, and why does it matter to me? *ResinDesigns Chase Corporation*, 2020.
- [7] Doyoung Jang, Dmitry Yakimets, Geert Eneman, Pieter Schuddinck, Marie Garcia Bardon, Praveen Raghavan, Alessio Spessot, Diederik Verkest, and Anda Mocuta. Device exploration of nanosheet transistors for sub-7-nm technology node. *IEEE Transactions on Electron Devices*, 64(6):2707–2713, 2017.
- [8] Jaroslav Kováčik. Correlation between young’s modulus and porosity in porous materials. *Journal of Materials Science Letters*, 18:1007–1010, 07 1999.
- [9] Joris Lacord, Gérard Ghibaudo, and Frédéric Boeuf. Comprehensive and accurate parasitic capacitance models for two- and three-dimensional cmos device structures. *IEEE Transactions on Electron Devices*, 59(5):1332–1344, 2012.
- [10] Khwang-Sun Lee and Jun-Young Park. Inner spacer engineering to improve mechanical stability in channel-release process of nanosheet fets. *Electronics*, 10:1395, 06 2021.
- [11] Junjie Li, Yongliang Li, Na Zhou, Wenjuan Xiong, Guilei Wang, Qingzhu Zhang, Anyan Du, Jianfeng Gao, Zhenzhen Kong, Hongxiao Lin, Jinjuan Xiang, Li Chen,

- Xiaogen Yin, Xiaolei Wang, Hong Yang, Xueli Ma, Jianghao Han, Jing Zhang, Tairan Hu, and Henry Radamson. Study of silicon nitride inner spacer formation in process of gate-all-around nano-transistors. *Nanomaterials*, 10:793, 04 2020.
- [12] N. Loubet, S. Kal, C. Alix, S. Pancharatnam, H. Zhou, C. Durfee, M. Belyansky, N. Haller, K. Watanabe, T. Devarajan, J. Zhang, X. Miao, M. Sankar, M. Breton, R. Chao, A. Greene, L. Yu, J. Frougier, D. Chanemougame, K. Tapily, J. Smith, V. Basker, A. Mosden, P. Biolsi, T. Q. Hurd, R. Divakaruni, B. Haran, and H. Bu. A novel dry selective etch of sige for the enablement of high performance logic stacked gate-all-around nanosheet devices. In *2019 IEEE International Electron Devices Meeting (IEDM)*, pages 11.4.1–11.4.4, 2019.
- [13] MatWeb. Overview of materials for polytetrafluoroethylene (ptfe), extruded. https://www.matweb.com/search/datasheet_print.aspx?matguid=4e0b2e88eeba4aaeb18e8820f1444cdb.
- [14] Groppo E. Molinaro S., Cascianelli S. and De Filippo R. Soi mosfet process design and simulation (100 nm n-type). *Integrated Systems Techonolgy Project, Politecnico di Torino*, 2021.
- [15] University of Birmingham. What does the young’s modulus tell us about a material? <https://www.birmingham.ac.uk/teachers/study-resources/stem/physics/youngs-modulus.aspx>.
- [16] M. Pelosi. From finfet to nanosheet si-sige gaafet: fabrication process simulation and analysis. *Master Thesis*, 2021.
- [17] polymerdatabase.com. Dielectrical constants of polymers. <https://polymerdatabase.com/polymer%20physics/Epsilon%20Table.html>.
- [18] QuantumATK. Analyzing the thermo-mechanical properties of a polymer material, version: S-2021.06. https://docs.quantumatk.com/tutorials/crosslink_analysis/crosslink_analysis.html.
- [19] QuantumATK. Dielectrictensor. <https://docs.quantumatk.com/manual/Types/DielectricTensor/DielectricTensor.html>.
- [20] QuantumATK. Polymer builder, version: Q-2019.12. https://docs.quantumatk.com/tutorials/polymer_builder/polymer_builder.html.
- [21] QuantumATK. Quantumatk software solution for advanced semiconductor development. <https://www.synopsys.com/content/dam/synopsys/silicon/quantum-atk/pdf/qatk-datasheet-solution-for-semiconductors.pdf>.
- [22] QuantumATK. Specificheatcapacity. <https://docs.quantumatk.com/manual/Types/SpecificHeatCapacity/SpecificHeatCapacity.html>.

- [23] Donghyun Ryu, Ilho Myeong, Jang Kyu Lee, Myounggon Kang, Jongwook Jeon, and Hyungcheol Shin. Investigation of gate sidewall spacer optimization from off-state leakage current perspective in 3-nm node device. *IEEE Transactions on Electron Devices*, 66(6):2532–2537, 2019.
- [24] Krishna Saraswat. Low- κ dielectrics, department of electrical engineering stanford university. <https://web.stanford.edu/class/ee311/NOTES/Interconnect%20Lowk.pdf>.
- [25] L. Scognamiglio. 3d junctionless-fet technology: A comparative tcad simulation study with finfet and nsgaafet. *Master Thesis*, 2022.
- [26] Synopsys Sentaurus. Sentaurus tcad industry-standard process and device simulators. https://www.synopsys.com/content/dam/synopsys/silicon/datasheets/sentaurus_ds.pdf.
- [27] D Shamiryan, T Abell, F Iacopi, and K Maex. Low- κ dielectric materials. *Materials Today*, 7(1):34–39, 2004.
- [28] Yabin Sun, Hengbin Gao, Shaojian Hu, Ziyu Liu, Xiaojin Li, Yun Liu, and Yanling Shi. Sub-thz small-signal equivalent circuit model and parameter extraction for 3 nm gate-all-around nanosheet transistor. *Processes*, 10:1198, 06 2022.
- [29] Meng Xie, Menglu Li, Quan Sun, Wenjie Fan, Shuang Xia, and Wenxin Fu. Research progress on porous low dielectric constant materials. *Materials Science in Semiconductor Processing*, 139:106320, 2022.